Revisiting silicate authigenesis in the Pliocene–Pleistocene Lake Tecopa beds, southeastern California: Depositional and hydrological controls

Daniel Larsen*
Department of Earth Sciences, University of Memphis, Memphis, Tennessee 38152, USA

ABSTRACT

The Pliocene–Pleistocene Lake Tecopa beds present a well-documented example of authigenic silicate diagenesis in an ancient saline, alkaline lake environment. Controls on authigenic mineral formation and distributions were investigated in nine stratigraphic sections aligned along a north-south transect in the Tecopa basin. Specifically, potential depositional and hydrologic controls on mineral assemblages and distributions were addressed by correlating detailed sedimentological data and basin hydrology with authigenic mineral facies distributions.

Deposition occurred within the Lake Tecopa basin in environments ranging from alluvial and eolian around the basin margin to lake margin, mudflat, and shallow and perennial lacustrine in the basin center. The authigenic silicate minerals include trioctahedral smectite, phillipsite, clinoptilolite, opal C-T (cristobalite-tridymite), potassium feldspar, illite, albite, and searlesite, as well as many other minor or less commonly observed phases. Authigenic mineral distributions along the margin of the basin are strongly controlled by sediment composition (primarily tuffaceous component) and lake-level variations. Authigenic mineral compositions in the center of the basin are dominated by feldspar, illite, and searlesite, and are less influenced by sediment composition or short-term changes in lake level. The authigenic silicate mineral composition in the central part of the basin is interpreted to be a result of chemical interaction with a saline, alkaline brine that moved in accord with lake-level changes and induced density-driven circulation. The results suggest that distributions of authigenic silicate minerals in saline, alkaline lake deposits are complexly related to depositional and hydrologic processes and may be of limited utility in resolving lake-level changes in ancient lacustrine systems.

Keywords: saline, alkaline lake, Pliocene–Pleistocene, zeolite, depositional facies, authigenic minerals.

INTRODUCTION

The Pliocene–Pleistocene Lake Tecopa beds represent a classic example of concentric distributions of authigenic silicate minerals (Fig. 1) attributed to diagenetic reactions in saline, alkaline lake deposits (Hay, 1966; Sheppard and Gude, 1968, 1969, 1973; Surdam and Parker, 1972). Past studies of silicate authigenesis in saline, alkaline lake deposits have largely focused on the types and distributions of zeolites (Sheppard and Gude, 1968, 1973; Surdam and Parker, 1972; Ratterman and Surdam, 1981; Sheppard, 1994) and pore-water chemistry (Jones, 1966; Eugster, 1970; Surdam and Eugster, 1976; Eugster and Hardie, 1978; Taylor and Surdam, 1981). Several studies, mainly from East Africa, have attempted to establish relationships, if present, between specific sedimentary facies in basins containing saline, alkaline lake deposits and their authigenic silicate mineralogy (Hay, 1976; Bellanca et al., 1992; Renaut and Tiercelin, 1994; Ingles et al., 1998; Deocampo and Ashley, 1999; Ashley and Driese, 2000; Hay and Kyser, 2001; Hover and Ashley, 2003). Because distributions and types of sedimentary facies in lake basins are fundamentally related to basin hydrology and climate (Smoot and Lowenstein, 1991; Rosen, 1994), relationships between sedimentary facies and authigenic mineral distributions provide information regarding hydrological processes in saline, alkaline lake basins and, indirectly, paleoclimatic conditions.

In this study, the stratigraphy and authigenic mineralogy of the Pliocene–Pleistocene Lake Tecopa Beds were examined to assess the varying roles of sedimentary, chemical, and hydrological processes in controlling the types and distributions of authigenic minerals. The incised badlands exposures in the Tecopa basin provide relatively easy lateral correlation of beds (especially marker beds) and three-dimensional analysis of lateral facies variations. The hyperarid climate of the southwestern Great Basin has preserved much of the authigenic mineralogy, although the most soluble salts, such as halite and trona, are largely absent from surface exposures due to dissolution during weathering. The stratigraphic and mineralogical results are used to (1) construct a conceptual model emphasizing controls on authigenic silicate distributions in saline, alkaline lake deposits, and (2) discuss the paleohydrologic and paleoclimatic information recorded by authigenic silicate distributions in such deposits.

AUTHIGENIC SILICATE MINERAL DISTRIBUTIONS IN SALINE, ALKALINE LAKES

In most cases, saline lake basins are partially or completely hydrologically closed all or most of the time, so that evaporation leads to formation of concentrated water compositions that may ultimately become brines (Jones, 1966; for a review, see Jones and Deocampo, 2003). The chemical evolution of evaporating waters is most sensitive to the balance of Ca^{2+} and bicarbonate contents (Ca^{2+}-HCO_3–chemical divide; Hardie and Eugster, 1970). Water compositions in which the bicarbonate equivalents exceed the calcium equivalents ($2m_{HCO_3^-} > m_{Ca^{2+}}$) lead to calcium-poor, bicarbonate-rich water compositions during evaporation and associated precipitation of calcium carbonate. Because Mg carbonates do not precipitate readily, bicarbonate concentrations increase with evaporation until oversaturation with alkali–alkali earth carbonates and bicarbonates (e.g., gaylussite, trona) is reached (Eugster and Hardie, 1978). Assuming that the pH is controlled by the carbonate system, the pH increases through evaporative concentration of such waters until bicarbonate mineral precipitation and hydrolysate complexation (e.g., silicic acid) buffer the pH (Eugster, 1980).

*dlarsen@memphis.edu

Geosphere; June 2008; v. 4; no. 3; p. 612–639; doi: 10.1130/GES00152.1; 11 figures; 2 tables; 2 plates.

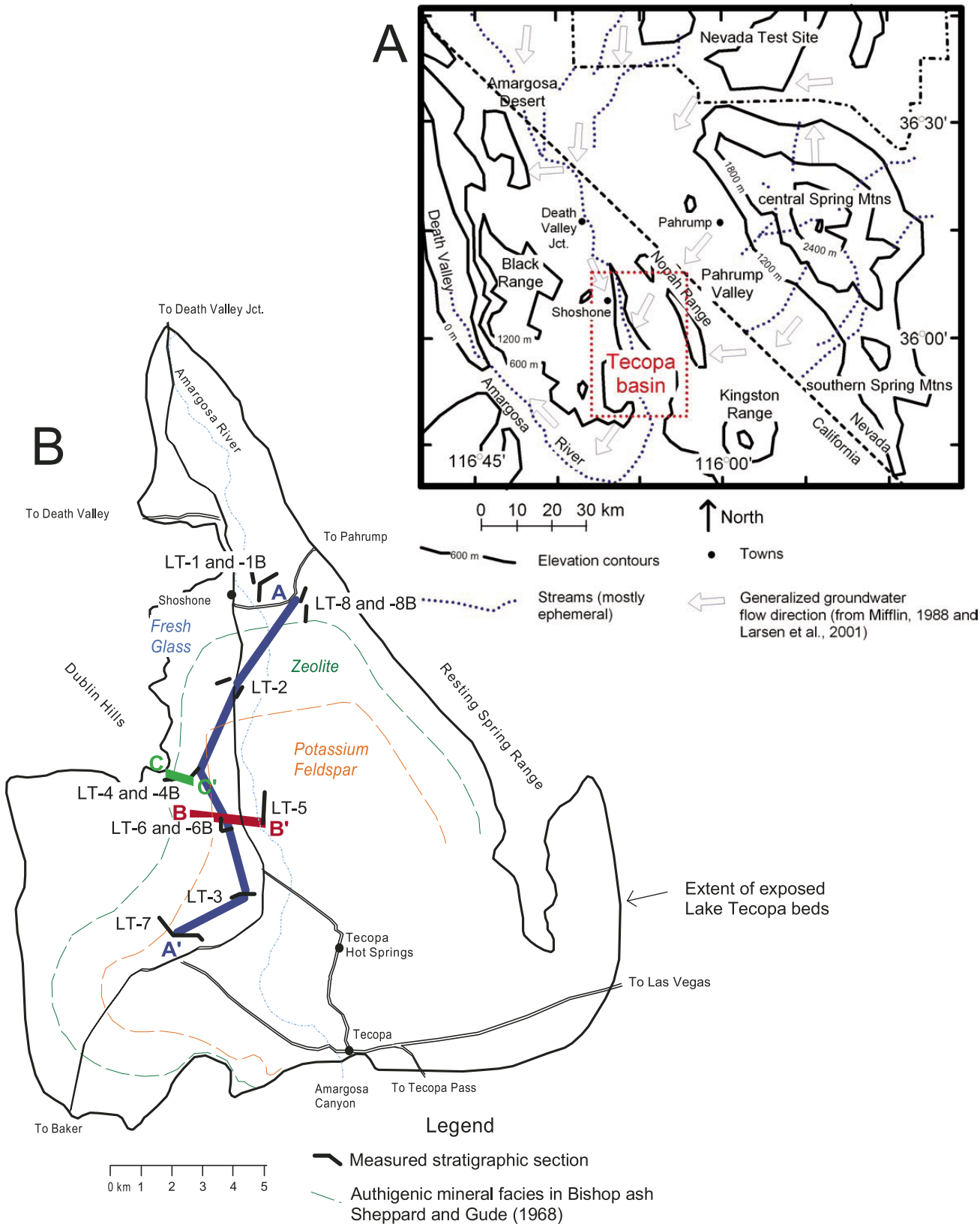

Figure 1. (A) Map of region surrounding the Tecopa basin, illustrating mountains, streams, and general groundwater flow directions. (B) Map of the Tecopa basin illustrating the locations of measured stratigraphic sections and correlated sections (line A-A' in Plates 1 and 2, line B-B' in Figs. 3 and 9, and line C-C' in Fig. 10). Note that line A-A' in Plate 2 includes section LT-1 rather than LT-8. Also shown are the authigenic mineral facies identified in the B tuff by Sheppard and Gude (1968).

The unique combination of evaporative concentration and bicarbonate-rich water compositions in saline, alkaline lakes leads to conditions favoring rapid hydrolysis of labile silicate minerals and volcanic glass (Hay, 1966). The resulting high pH water (pH commonly >9) leads to solubilization of silica and aluminum from relatively unstable mineral phases, which subsequently drives chemical oversaturation of the water with stable minerals such as quartz, alkali feldspar, and muscovite. In saline, alkaline lakes, the stable minerals cannot precipitate quickly enough to keep pace with evaporation and hydrolysis; thus, precipitation of metastable zeolite and clay mineral phases from gels partially decreases the chemical energy of the system (Dibble and Tiller, 1981). Ultimately, the stable minerals, such as quartz, alkali feldspar, and muscovite, are believed to replace the earlier formed zeolites and clays. Zeolites are not extensively preserved in saline, alkaline lake deposits older than Mesozoic age (Hay, 1966; Langella et al., 2001). This is presumably due to factors such as dissolved silica content, temperature, and Ostwald ripening (Surdam and Sheppard, 1978; Dibble and Tiller, 1981; Chipera and Apps, 2001).

The primary control on the distribution of clay minerals and zeolites in saline, alkaline lake settings is thought to be spatial variations in water chemistry imposed by closed-basin hydrology (Fig. 2) (Jones, 1966; Surdam and Sheppard, 1978). Other factors, such as cationic ratios and pH of pore water during mineral precipitation, labile phase composition (e.g., detrital clays, volcanic glass), and temperature, provide secondary controls on the types of minerals formed (Surdam and Eugster, 1976; Surdam and Sheppard, 1978; Chipera and Apps, 2001; Deocampo et al., 2002; Hover and Ashley, 2003). However, lake levels in hydrologically closed basin are seldom stable (Langbein, 1961) and, because of this fact, are often used as indicators of paleoclimatic change (Street-Perrott and Harrison, 1985; Cohen, 2003). Based on this reasoning, variations in lake level, or more specifically lake surface area, should also affect in a systematic manner clay mineral and zeolite distributions through time, assuming that all other factors are equal.

STUDY AREA

The Pliocene–Pleistocene Lake Tecopa Beds (Allogroup of Morrison, 1999) of southeastern California (Fig. 1) are a Pliocene–Pleistocene basin-fill sequence that has been extensively dissected by late Pleistocene incision of the Amargosa River (Morrison, 1991, 1999). Prior to middle or late Pleistocene breaching of the Tecopa basin, Lake Tecopa was the terminal lake for discharge of the ancestral Amargosa River during Quaternary and late Tertiary time (Dohrenwend et al., 1991; Morrison, 1999). The general stratigraphy of the deposits was established by Sheppard and Gude (1968) and Hillhouse (1987), and refined by Morrison (1991, 1999) and Larsen (2000). Dating of the Lake Tecopa beds is mainly based on numerous volcanic ash beds, six of which have been correlated to well-dated volcanic events (Sarna-Wojcicki et al., 1987). The Tecopa beds have also been the subject of numerous paleomagnetic investigations (Hillhouse, 1987; Valet et al., 1988; Larson and Patterson, 1993), although silicate mineral authigenesis appears to limit the temporal resolution of this technique. Invertebrate fossils are rare, but vertebrate remains are present in numerous localities (Reynolds, 1991; Woodburne and Whistler, 1991). In terms of tectonic activity, the Tecopa basin has been relatively stable throughout the Quaternary, although warping within and around the margins of the basin has caused local deformation (Morrison, 1999) and may have influenced the basin overflow history (Larsen et al., 2003).

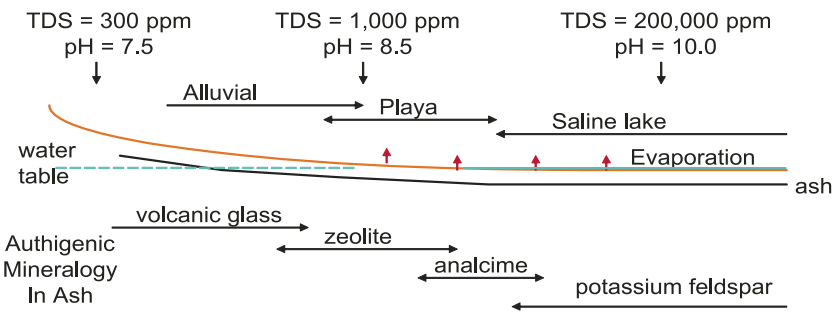

Figure 2. Diagrammatic cross section of saline, alkaline lake basin showing mineralogical changes in an ash bed having interacted with fresh to saline, alkaline waters (from Surdam and Sheppard, 1978). TDS—total dissolved solids.

METHODS

Stratigraphic sections were measured in areas with moderate to good exposure and were trenched or scraped to reveal stratigraphic detail. Samples for mineralogical analysis were collected on a meter to submeter scale in the sections, depending on the degree of lithologic variability. The samples were split visually into representative fractions for X-ray diffraction (XRD), petrographic, and scanning electron microscope (SEM) analysis.

Samples for XRD analysis were initially crushed to disaggregate the sample and then ground to a fine powder using a mechanical mortar and pestle. Bulk sample powder was quantitatively mixed with crystalline CeO_2 mineral standard using a 9:1 ratio of sample to standard. Mineral standards for most phases present in the Lake Tecopa beds were prepared with CeO_2 to establish reference intensity ratios for qualitative mineral analysis. Samples and standards were analyzed using a Philips 1710 diffractometer with Cu K_α X-ray radiation from 3° to 63° 2θ; step increment and step time were 0.05° 2θ and 3 s, respectively.

Samples analyzed for clay mineralogy were first processed to remove calcium carbonate using 5 N acetic acid buffered to pH = 5 and subsequent deionized water rinses (Moore and Reynolds, 1989). Oven-dried sample weight before and after carbonate removal was determined to provide an estimate of carbonate (and soluble salt) loss. The dried sample was recrushed and added to a 10% sodium pyrophosphate solution, disaggregated for 3 min in a sonic dismembrator, and centrifuged for 6 min and 40 s to obtain a sample of the <2 μm clay-size mineral fraction. The clay fraction was saturated with 1 M $MgCl_2$ solution and mounted on a glass slide using the Millipore method (Drever, 1973). The oriented clay mounts were run both air dried and after solvation with ethylene glycol. Samples and standards were analyzed using a Philips 1710 diffractometer with Cu K_α X-ray radiation from 3° to 35° 2θ; step-increment and step time were 0.04° 2θ and 3 s, respectively. XRD analysis of a randomly oriented mount of the [060] diffraction peak was attempted (e.g., Deocampo, 2004); however, the peaks were of low magnitude and quantification of trioctahedral and octahedral clay mineral fractions was not possible.

Petrographic thin sections were prepared for several samples; however, the authigenic mineral relationships were typically too fine to resolve accurately with a polarized-light microscope. Sample chips were mounted for scanning electron microscopy and coated with gold and palladium. A Philips XL30 ESEM was operated

using an accelerating voltage between 15 and 30 KeV and a sample current of 20 ma. Qualitative chemical compositional analysis was obtained using an energy dispersive X-ray analysis system (EDAX).

STRATIGRAPHY

To date, 12 detailed stratigraphic sections have been measured. Most of the sections are located along the central axis of the Tecopa basin (Fig. 1 and Plate 1), although shorter sections have also been measured along the basin margin in several locations. Following the practice of other workers (Morrison, 1991, 1999; Hillhouse, 1987), the three major tuffs (Lava Creek B, Bishop, and Huckleberry Ridge) are used for correlation of the sections across the basin. Other tuffs and lithologically distinct mudstones are used to correlate basin-center to basin-margin sections.

The correlated stratigraphic sections (Plate 1 and Fig. 3) reveal sandy to gravelly basin-margin sections correlating to finer grained basin-center sections. The basin-center sections are also somewhat thinner than correlative basin-margin sections, presumably due to greater compaction of the finer grained basin-center deposits. Because of deeper incision and more complete excavation of the basin-center region, the Bishop tuff and enclosing deposits are better represented near the margins, whereas the Huckleberry Ridge tuff and enclosing deposits are better represented in the basin center. The lower age limit of the exposed deposits is unknown, but is thought to be at least 2.5 Ma based on paleomagnetic analysis (Larson et al., 1991). The upper age limit is also unknown, but is bracketed by spring deposits located in the northern part of the basin (Fig. 1) that contain an ash interpreted to be the 0.2 Ma Wadsworth(?) ash (Morrison, 1999; Sarna-Wojcicki et al., 1987). In contrast to Morrison (1999), who interpreted the Wadsworth(?) ash and enclosing beds to be conformable lake-margin strata within the Lake Tecopa beds, the Wadsworth(?) ash and enclosing silty beds are here interpreted to be silt and ash deposited unconformably on the Lake Tecopa beds near paleosprings aligned along the northeastern part of the basin (see Nelson et al., 2001). Similar types of spring deposits are observed throughout the southern Great Basin (Quade et al., 1995; Jeff Knott, 2003, personal commun.) and have caused interpretive problems in the past.

DEPOSITIONAL FACIES

The depositional facies in the Lake Tecopa beds include a variety of mudstone, siltstone, sandstone, conglomerate, tuff, and tufa (subaerial and freshwater limestone). Many of the fine-grained sedimentary facies are tuffaceous, but the coarser-grained facies are composed of epiclastic detritus derived from local bedrock and the ancestral Amargosa River drainage basin. A silt-sized detrital component is common in fine-grained subaerial deposits and locally forms loess deposits, indicating that eolian detritus is an important sedimentary component in the basin. Trace fossils are abundant in the terrestrial and lacustrine-margin facies and guide paleoenvironmental interpretations. The subaerial deposits are generally weakly consolidated (mainly due to calcite cement) or unconsolidated, whereas the lacustrine deposits are consolidated and cemented by clay minerals, zeolites, and other fine-grained silicate minerals (Sheppard and Gude, 1968).

Depositional Environments

The depositional facies and their distribution in the Lake Tecopa beds are interpreted in terms of eight depositional environments. Examples of stratigraphic intervals representing these environments are illustrated in Plate 1 and Figure 3.

Perennial Lacustrine

The relatively deep water lacustrine environment is dominated by diagenetically altered mudstone with common pores and calcite-filled casts remnant of gaylussite. Light gray and greenish-gray to pinkish-gray mudstones with common to abundant centimeter-sized pores, some in the shape of euhedral gaylussite crystals, and containing flame structures and soft-sedimentary deformation are interpreted to be perennial lacustrine deposits. At one location (section LT-5, 17 m), calcite pseudomorphs after radiating, bladed trona crystals are preserved in the mudstone (Fig. 4A). White, light gray, or light reddish-brown fine ash tuff is commonly interbedded with mudstone in massive or 1–50-cm-thick beds with rare to common light gray to greenish-gray siliceous nodules, and millimeter- to centimeter-scale pores. Meter-scale ball and pillow soft-sediment deformation (Fig. 4B) is present in some tuff and tuffaceous sandstone. Tuff within the lacustrine deposits is typically dense with extensive zeolite or potassium feldspar alteration (Sheppard and Gude, 1968).

The mud is interpreted to have settled from the water column during fair weather conditions. Wave-worked sand is generally not present, although muddy very fine grained sand is locally present and probably represents subaqueous fallout from hyperpycnal flows. Similar types of flows laden with ash augmented the fallout distribution of ash to form the tuff beds. Gaylussite and trona grew displacively in the lake muds by chemical reactions with sodium-carbonate brine, much as they do currently in Lake Bogoria, East Africa (Renaut and Tiercelin, 1994). Siliceous nodules in tuffaceous intervals are interpreted to be associated with diagenetic alteration of magadiite cherts, similar in shape and surface texture to those observed at Lakes Magadi and Natron in East Africa (Hay, 1968; Eugster, 1980) and locations in the western U.S. (Gude and Sheppard, 1986). Magadiite is present in some mudstone samples from the Lake Tecopa beds (Starkey and Blackmon, 1979). The absolute depth of the water cannot be determined, but this environment was distant from sand sources and was probably at least 5–10 m deep.

Shallow-Water Lacustrine

The shallow-water lacustrine environment is characterized by interbedded mudstone and laminated or wave-ripple cross-laminated very fine to fine-grained sandstone and tuff. The sandstones are light gray to light brownish gray, generally very fine to medium-grained, moderately sorted, and have planar bedding, cross-bedding, or wave-ripple cross-lamination. The tuff is white, light gray, or light reddish brown and fine to medium bedded, commonly with wave-ripple cross-lamination (Fig. 4C). The sandstone and tuff also have common to abundant millimeter-size pores and extensive diagenetic alteration. The mudstones are light gray to pinkish gray and have common to abundant fine millimeter-sized pores and rare root traces. Irregularly shaped siliceous nodules, 5–10 cm across, and complete silica replacement (Fig. 4B) are common in some of these beds.

Wave-rippled sandstone beds are typically <5 cm thick and in very thin beds that represent individual bedforms. These sandstone beds are interpreted as sands that were transported to shallow lacustrine environments during storms or from flood-related turbid flows and then reworked into wave ripples during subsequent fairweather conditions. The mudstone was deposited during low wave-energy conditions adjacent to marshy areas along the shore and in offshore areas. The mudstone and sandstone commonly contain centimeter- to millimeter-sized pores, either from dissolved evaporite minerals, such as gaylussite, or gas accumulation. The degree of tuffaceous bed replacement by magadiite chert is more extensive in shallow lacustrine facies than in perennial lacustrine facies, presumably driven by leaching of sodium from dilute runoff along the lake margin (Eugster, 1980).

Lacustrine Margin

The lacustrine-margin environment is characterized by sandstone and mudstone that contain

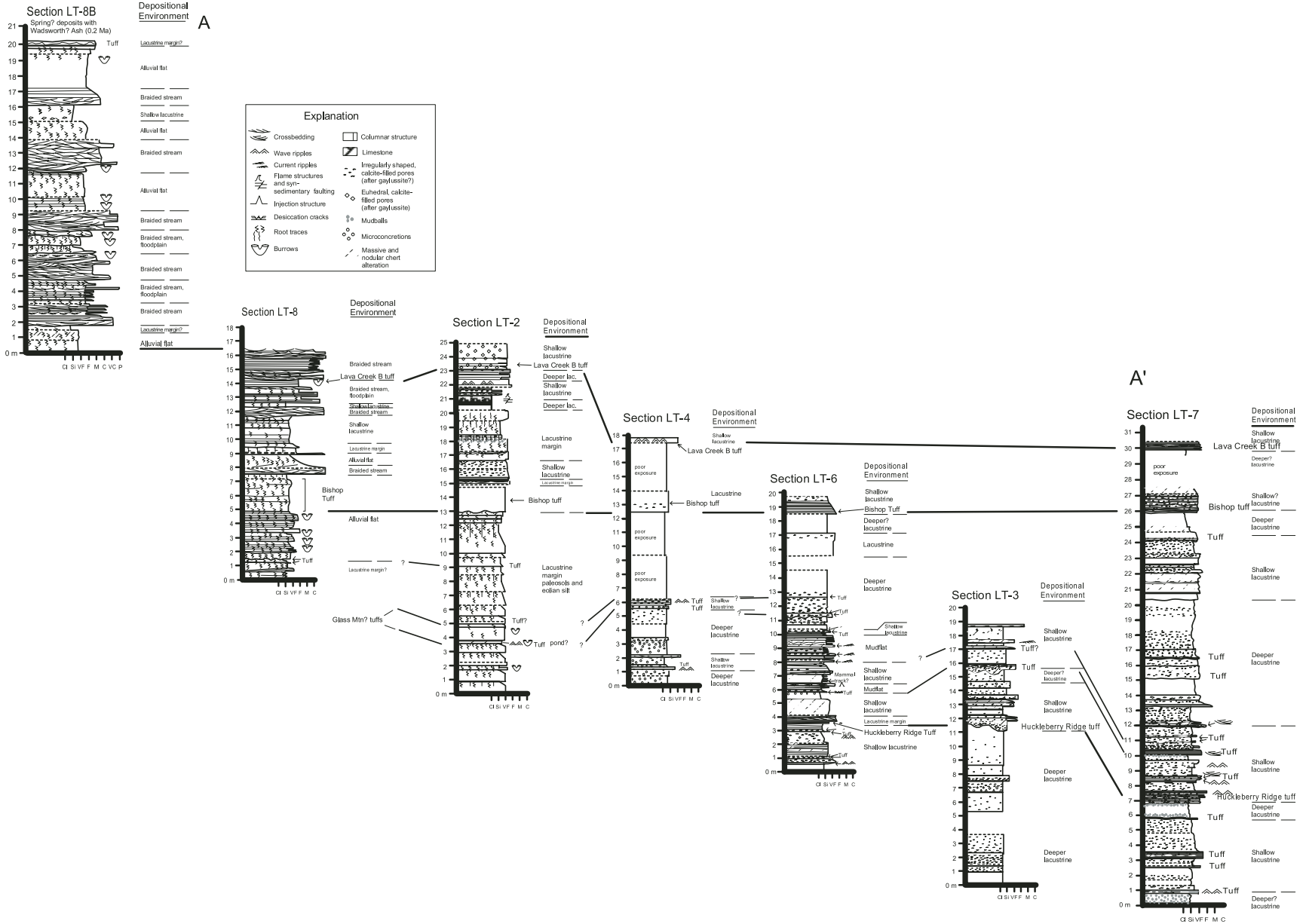

Plate 1. Correlated sections along line A-A' in Figure 1. Depositional environments are discussed in the text. Cl—clay; Si—silt; VF—very fine-grained sand; F—fine-grained sand; M—medium-grained sand; C—coarse-grained sand; VC—very coarse-grained sand; P—pebbles. If you are viewing the PDF of this paper or reading it offline, please visit http://dx.doi.org/10.1130/GES00152.SP1 (Plate 1) or the full-text article on www.gsajournals.org to view Plate 1.

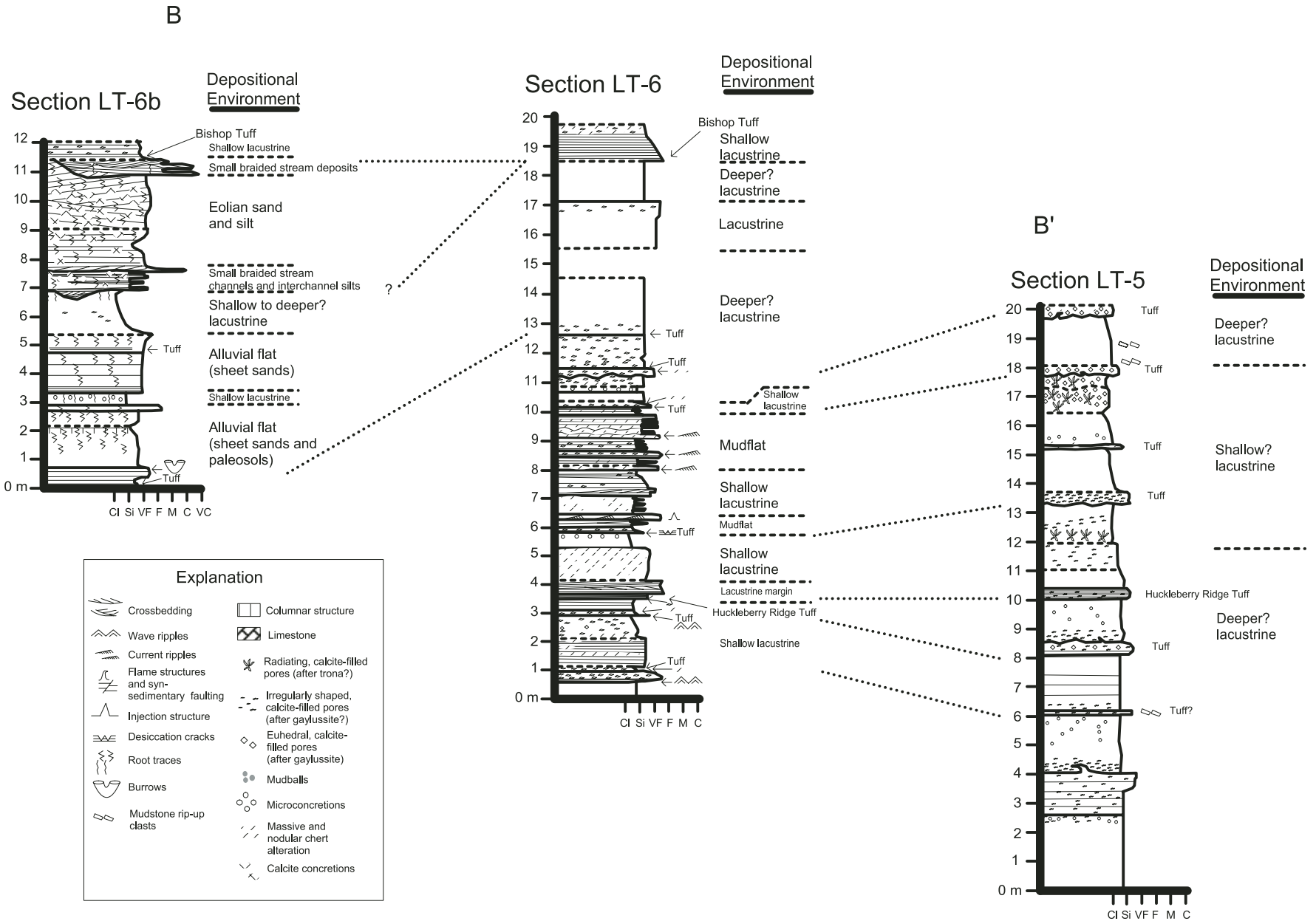

Figure 3. Correlated sections along line B-B' in Figure 1. Depositional environments are discussed in the text. Cl—clay; Si—silt; VF—very fine-grained sand; F—fine-grained sand; M—medium-grained sand; C—coarse-grained sand; VC—very coarse-grained sand.

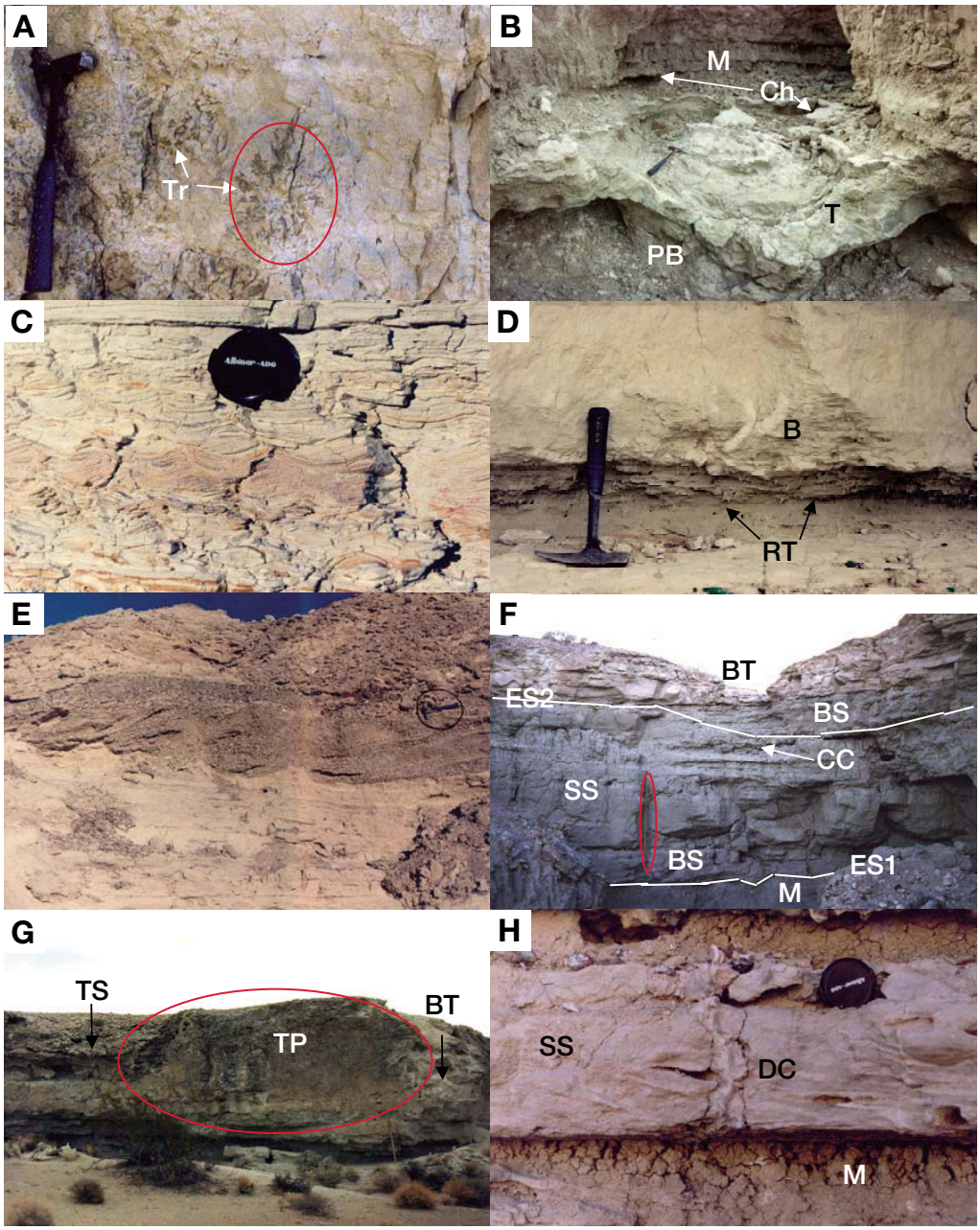

Figure 4. Photographs of depositional facies discussed in the text. (A) Perennial lacustrine environment: mudstone with radiating calcite pseudomorphs after trona (Tr); section LT-5, 17 m. (B) Perennial lacustrine to shallow lacustrine environment: altered Huckleberry Ridge tuff (T) interbedded with mudstone and cherty mudstone (M), overlain by shallow-lacustrine siltstone and very fine-grained wave-rippled sandstone; section LT-3, 11–13 m. Tuff foundered into underlying lake muds to form ball-and-pillow structure (BP). Chert (Ch) replaces tuff and mudstone. (C) Shallow lacustrine environment: ripple cross-laminated Lava Creek B tuff; section LT-2, 22.2 m. Lens cap is ~7 cm across. (D) Lacustrine-margin (deltaic) environment: cross-laminated sandstone overlain by sandy mudstone with subvertical burrows (B) and gypsum-filled root traces (RT); section LT-1, 2.5 m. Rock hammer is ~32 cm long. (E) Lacustrine-margin to perennial stream environment: horizontal-bedded to ripple cross-laminated medium-grained sandstone (alluvial-flat and deltaic environment) overlain by cross-bedded to horizontal-bedded pebbly perennial-stream conglomerate; section LT-1, 20–22 m. Conglomerate fills channel scour in underlying sheet delta sandstone. Rock hammer, ~32 cm long, circled for scale. (F) Lacustrine, alluvial-flat, and eolian environments: Greenish-gray lacustrine mudstone (M) with erosional upper surface (ES1) overlain by low-angle cross-bedded ephemeral-stream sandstone (BS) of the alluvial-flat environment, that grade upward into silty, very fine-grained eolian sandstone (SS) with horizontal beds to low-angle cross-bedding and centimeter-size calcite concretions (CC). Another erosional surface (ES2) truncates the eolian sandstone and is filled by more low-angle cross-bedded alluvial-flat sandstone, which is followed by altered shallow-lacustrine Bishop tuff (BT) with diagenetic pores and crude 10-cm-scale beds; section LT-6B, 19–24 m. 1.8 m staff is circled in red. (G) Lacustrine-margin environment: tufa pillow (TP, circled in red) overlying deformed Bishop tuff (BT); section LT-1, 13–16 m. Note tuffaceous sandstone (TS) fills between tufa pillows. Staff is 1.8 m long. (H) Mudflat environment: interbedded mudstone (M) and ripple cross-laminated to horizontal-laminated fine- to medium-grained sandstone (SS); section LT-6, 6–6.5 m. Desiccation crack (DC) cuts through sandstone. Lens cap is ~7 cm across.

evidence for nearshore, shoreline, marsh, and deltaic sedimentation. The sandstones are light gray to light brownish gray, contain common to abundant root traces, and vertical to subvertical centimeter-diameter burrows (Figs. 4D, 4E). Sandstone with moderate sorting and planar bedding, low-angle cross-bedding, or ripple cross-lamination represents deposits of perennial stream and deltaic processes (Fig. 4E). Locally, pebbly very coarse grained sandstone with tabular cross-bedding and grain coatings represents wave-formed lacustrine bars and beach deposits (see Morrison, 1999). Light gray to greenish-gray mudstones with common to abundant root traces and rare vertical to subvertical centimeter-diameter burrows (Fig. 4D) are interpreted to be paleosols, whereas mudstones with common root traces, especially strongly vertical root traces (phreatophytes?), and fine millimeter-sized pores, presumed to be diagenetic molds, are interpreted to be marshy, lacustrine-margin deposits. The paleosols commonly exhibit prismatic columnar structure, and carbonate and clay accumulation along ped and pore surfaces, consistent with immature to moderately developed vertic paleosols. A few of the paleosols have prominent slickenslides, up to stage II carbonate accumulation ($CaCO_3$ films, root casts, and nodules) (Birkeland, 1999), and clay accumulation similar to buried Vertisols described by Gustavson (1991). The greenish-gray color and yellow, jarosite(?) root-trace filling suggest reducing conditions consistent with a high water table and protracted periods of saturation. White to light gray tuff with fine millimeter-sized pores commonly has current-ripple cross-lamination (Fig. 4C), 1–10-cm-thick horizontal bedding (Fig. 4F), or wave-ripple cross-lamination along with minor root traces. Truck-sized pillows of tufa are interbedded with planar-bedded to low-angle cross-bedded sandstone and lacustrine-margin mudstone in the axis of the basin east of Shoshone (Fig. 4G). The pillows have little internal structure and are composed of dense laminated to massive limestone. In Figure 4G, the underlying Bishop tuff beds are deformed by the pillows and overlying tuffaceous sandstone fills between pillows.

Nearshore and shoreline environments are indicated by winnowed, cross-bedded, pebbly sandstone, commonly with coated grains, that represent shallow lacustrine bars and beach foresets (see Morrison [1999] for a discussion of beach deposits). Marsh environments are indicated by mudstone and sandstone with common millimeter-sized diagenetic pores, vertical burrows, and root traces. Parts of sandstone beds that are not bioturbated are typically wave-ripple cross-laminated. The root traces are commonly vertical, suggesting shallow groundwater conditions. These deposits show variable degrees of diagenetic alteration.

Deltaic environments are represented by horizontal and low-angle cross-bedded sandstone, climbing ripple cross-laminated sandstone, and silty mudstone, all with variable amounts of root traces and vertical to subvertical burrows. Good examples of this facies are observed in the lower part of section LT-1 (Plate 1). These beds are commonly arranged in tabular to lensoid, fining-upward sequences, suggesting crude lobe development and abandonment. At section LT-1, the ripple cross-lamination foresets climb to the south, consistent with discharge of sediment-laden Amargosa River water into the lake. Silty drapes over sandstone laminae and beds are common and indicate slack-water deposition. The root traces are commonly filled with gypsum or jarosite(?), suggesting interaction with sulfate-rich groundwater. Large-scale clinoforms, typical of late Pleistocene deltaic deposits in other western U.S. lake basins (Born, 1972), are not observed. The character of the deposits suggests a wet sheet delta system similar to that described by Smoot and Lowenstein (1991) from Holocene Lake Cuahilla, southern California. The tufa deposits east of Shoshone likely formed from an ancestral Shoshone spring under rising lake-level conditions in a deltaic to nearshore environment.

Mudflat

The mudflat environment (Smoot and Lowenstein, 1991) is represented by interbedded cherty sandstone, siltstone, and mudstone with evidence for desiccation and dry conditions. The sandstone includes individual wave-ripple cross-laminated beds and lenses (as much as 20 cm high and 6 m across) with horizontal bedded and ripple cross-laminated beds. Mudcracks are observed in some thin alternating sandstone (Fig. 4H) and mudstone beds. In addition, mammal tracks, possibly of a camel, are observed in one thin sandstone bed. The extensive siliceous replacement is interpreted to be associated with magadiite precipitation by wetting and drying of the mudflat floor and subsequent opal C-T (cristobalite-tridymite) or quartz replacement.

Alluvial Flat

The alluvial-flat environment (sensu Mack et al., 1994) is characterized by interbedded sandy mudstone, typically with evidence for pedogenic modification, and crudely bedded sheetflood sandstone. Thin (<0.5 m) intervals of low-angle cross-bedded medium- to coarse-grained sandstone are locally present and represent small ephemeral stream channels (e.g., Picard and High, 1973). The crudely bedded sandstones are poorly sorted and bioturbated, consistent with deposition from sheet-like or poorly channelized flow across the alluvial-flat landscape. The sandy mudstone intervals are gray to pinkish gray and crudely bedded with abundant root traces and burrows, but rarely show color or ped structure consistent with paleosol development. The root traces are very fine to medium sized and are consistent with desert grasses and shrubs. Centimeter-sized burrows (generally nonmeniscate, vertical to subvertical, and either ~0.5 or 1–2 cm diameter) in the mudstone and sandstone are similar in size and form to a variety of beetle traces present in alluvial to marginal-lacustrine environments (Hasiotis, 2002).

Alluvial Fan

Alluvial-fan deposits have not been described in the sections measured to date, but are present in exposures west of Shoshone and along the southern margin of the basin. Alluvial-fan facies include interbedded poorly sorted conglomerate, moderately to poorly sorted sandstone, and siltstone. Basin-margin conglomerate is typically composed of angular to subangular, poorly sorted cobbles, pebbles, sand, and silt. This conglomerate is crudely bedded in tabular bodies and is interpreted as deposited by debris flows and sheet floods. Sandstone with poor sorting and crude centimeter-scale horizontal bedding or low-angle cross-bedding represents deposits of flood and ephemeral stream processes, respectively. The sandstone commonly grades upward into sandy and silty beds with evidence of pedogenic modification, including rubification, blocky ped structure, and carbonate nodules, root casts, and films (e.g., Birkeland, 1999).

The alluvial-fan environment is characterized by interbedded debris-flow conglomerate, sheetflood sandstone, cross-bedded ephemeral stream sandstone, and silty calcic paleosols. Conglomerate and pebbly sandstone fine down gradient (over distances of 100–200 m) into sandy, silty, or muddy deposits, which in some cases are laminated, undisturbed, and clearly lacustrine. The conglomerate and sandstone beds contain angular to subangular clasts with a more limited variety of clast compositions (mainly from Paleozoic carbonate and quartzite and Tertiary volcanic rocks surrounding the Tecopa basin) than ancestral deposits of the Amargosa River. Weakly cemented conglomerate and sandstone are often interbedded with tufa mounds (Nelson et al., 2001) and tufa-cemented sandstone and conglomerate, suggesting that spring discharge periodically affected fan deposition.

Perennial Stream

Perennial stream deposits are present east of Shoshone and reflect sedimentation by the

ancestral Amargosa River. Channel-fill conglomerate and scour-and-fill pebbly sandstone are inset into rooted and burrowed sandy siltstone and pebbly sheetflood sandstone (Fig. 4E). These deposits grade toward the margins into alluvial-flat deposits and toward the south into sheet-delta or other types of deltaic deposits. Tufa-cemented sandstone is also locally present and suggests that spring discharge periodically affected stream deposition.

Eolian Deposits

Loess deposits include massive silt, and eolian sand-dune deposits include low-angle cross-bedded, silty very fine- to fine-grained sand (Fig. 4F). Coarser sand and pebbles are absent from these beds, as are scour-and-fill structures. Both silt and fine sand beds show sparse to common fine-scale root traces, minor carbonate accumulation, and commonly have 1–20-cm-long, bedding-plane–parallel carbonate nodules, similar to those described by Mozley and Davis (2005) in the Neogene Santa Fe Group, New Mexico, USA, and centimeter-sized carbonate concretions.

Eolian silt and fine sand deposits aggraded where vegetation and moisture forced sedimentation. These deposits are present in strata exposed along the eastern margin of the Dublin Hills; however, abundant silt is common in paleosols throughout the basin, suggesting that eolian input was prominent basin wide. The elongate carbonate concretions in the eolian deposits have sharp contacts and parallel orientation, consistent with precipitation from groundwater during wetter conditions following deposition (e.g., Mack et al., 2000; Mozley and Davis, 2005).

Mineralogy

The bulk mineral composition of samples from the Lake Tecopa beds is tabulated in Table 1. The mineralogy of the Lake Tecopa beds includes detrital, depositional, and diagenetic components. The detrital minerals are present as individual grains and within polymineralic rock fragments. Many minerals such as quartz, Ca-Na plagioclase feldspar, and mafic silicate minerals are almost certainly detrital (Fig. 5A); these minerals are common in the unaltered, subaerial deposits. However, alkali feldspar and a variety of clay minerals, which may be authigenic, are also present in the subaerial deposits and are interpreted based on petrography and lack of cementation to be of detrital origin in these deposits as well. Depositional minerals are those that precipitate in the depositional environment, largely at or near the sediment-water interface. The only clearly depositional mineral present in the Lake Tecopa beds is calcite in the tufa deposits, and at least part of the calcite in those deposits may have precipitated following deposition (i.e., diagenetic).

Diagenetic authigenic minerals precipitate within sediments due to chemical reactions between pore water and sediment. In the Lake Tecopa beds, the diagenetic minerals exhibit interstitial (Fig. 5A), replacive (Fig. 5B), and displacive (Fig. 4A) growth patterns. Interstitial minerals precipitate from solution or unstable intermediates (nonminerals and gels) to fill void space between grains or previous cements. A good example is clay minerals precipitated between detrital grains in Figure 5A. Replacive minerals form within a dissolved or partially dissolved detrital grain from chemical elements originating in the dissolved grain and/or external to the grain. Zeolite or authigenic feldspars replacing volcanic glass in a shard is a typical example of replacive mineral growth in the Lake Tecopa beds (Fig. 5B). Displacive minerals form within unconsolidated sediments by pushing aside detrital grains during crystallization. Gaylussite and trona, which are no longer preserved but identified by calcite pseudomorphs and open molds in the Lake Tecopa beds, are interpreted to have grown displacively in some lacustrine mudstones (Fig. 4C).

Of primary interest in this study are the diagenetic minerals and specifically the authigenic silicates. XRD patterns for some authigenic minerals are distinct from those of detrital counterparts (e.g., authigenic potassium feldspar versus sanidine or microcline). However, petrography and scanning electron microscopy were used to confirm authigenic growth patterns in as many samples as was feasible. Previous studies have described most of the authigenic minerals observed in the present study (Sheppard and Gude, 1968; Starkey and Blackmon, 1979). Sheppard and Gude (1968) demonstrated authigenic growth relationships for the zeolites, searlesite, and authigenic potassium feldspar in tuffs. In contrast, Starkey and Blackmon (1979) argued that most clay minerals (aside from sepiolite) in the lacustrine mudstones and tuffs are detrital rather than diagenetic. The results from the present work suggest based on authigenic SEM textures and uniform clay composition that diagenetic clay minerals in all lacustrine facies are more common than discussed by Starkey and Blackmon (1979).

Zeolites

The most common zeolites encountered in this study are phillipsite, clinoptilolite, and analcime. Other zeolites observed with less frequency include chabazite, erionite, and mordenite. Phillipsite is observed in most facies and commonly forms elongate monoclinic prisms (Fig. 6A). Clinoptilolite is also observed in most types of facies and commonly forms thin, pseudorhombohedral crystals (Fig. 6B). Analcime is present in lacustrine and lacustrine-margin facies. Although analcime is most commonly present with authigenic potassium feldspar, it is also observed in reaction relationship with phillipsite or clinoptilolite (Fig. 6C). Erionite is present in trace quantities in most facies as a late-stage pore fill (Fig. 6D). Chabazite is present in trace quantities in facies from the center of the basin, although its paragenetic relationship to other authigenic minerals is uncertain.

Clay Minerals

The two major clay minerals are smectite and illite. Chlorite is present in trace quantities in a variety of facies, most likely as a detrital mineral given its typical metamorphic and marine sedimentary origins. Sepiolite and palygorskite (Fig. 6E) are present in minor to trace quantities along with smectite in a few lacustrine and lacustrine-margin samples. Smectite is present in both dioctahedral and trioctahedral forms as determined by peak position of the [060] peak. However, dioctahedral smectite is the dominant variety in the alluvial and alluvial-flat deposits, whereas trioctahedral smectite is the dominant variety in the lacustrine and lacustrine-margin facies (Fig. 6E). In alluvial and alluvial-flat deposits, smectite is observed to have a typical cornflake–type appearance (Fig. 5A), but vermicular or finely matted textures (Fig. 6A) are also observed. Illite is present in nearly pure form, showing little evidence of mixed layering with smectite. Illite is present in all facies, but is the most prominent clay mineral in most of the samples from the central part of the basin.

Other Authigenic Silicate Minerals

Authigenic potassium feldspar, searlesite, albite, and opal C-T are present in varying abundances. Authigenic potassium feldspar is present in samples from the central part of the basin. It is typically present as fine 1–3-μm-size monoclinic prisms, both as matrix replacement and pore lining (Fig. 6F). Searlesite, $NaBSi_2O_5(OH)_2$, is present in samples from the central part of the basin, especially in the lacustrine and lacustrine-margin facies. Searlesite is present as pore-lining, thin, broad-bladed crystals as long as 50 μm (Fig. 6G); however, it may also be present as finer-grained crystals in matrix. Authigenic albite is identified in several samples by XRD and typically accompanies authigenic potassium feldspar (Fig. 7); however, it is not unambiguously observed in SEM (Fig. 6H). Similarly, opal C-T is identified in several samples by XRD, but has not been positively identified in SEM.

TABLE 1: BULK AND CLAY MINERAL COMPOSITION

Sample	Ht. in section (m)	Munsell color	Lithology*	Bulk Mineralogy†				Mineral facies§	Clay Mineralogy			
				Abundant	Common	Minor	Trace		Abundant	Common	Minor	Trace
LT-1-1A	2.0	light gray	tuff. ss	Ab, Q		Mi	Sm	D		Sm, I	Cl	Chl
LT-1-1B	2.2	white	tuff. sltst	Ab, Cc	Q	Sm	Ha, Mi	D				
LT-1-2	7.0	white	glassy tuff	Glass		Cc, Q, Fd, Sm		D				
LT-1-3C	14.3	white	tuff	Cc		Fd, Q, Sm		D				
LT-1-4	13.7		ss	Ab, Q		Mi, Cc, Cl, Ph, Sm	Ha	D				
LT-1-5	17.6	light gray	tuff. sltst	Cc	Q, Fd	Sm, Mi	Cl, Chl, Ph, Ha	D			Sm, I	Cl, Ph
LT-1-6	27.2	very pale brown	sandy tufa	Cc	Fd, Q	Mi, Sm	OC-T, Chl			Sm	I	Ph
LT-1-7	27.7	white	silty ss	Cc	Ab, Kf, Q	Mi, Sm	Cl	D				
LT-1-8	24.8	very pale brown	ss	Cc	Q, Fd	Mi, Sm	Gyp	D				
LT-2-1	3.5	light gray	tuff. sltst	Cc, Q	Ab, Sm	Mi, Ha, OC-T		D				
LT-2-2	4.5	white	tuff. ss	Cc	Q, Sm		Ha	D	Sm	Cl, Ph	I	Se
LT-2-3	5.1	white	tuff. ss	Cc	Sm, Q, Ab		Ha	D				
LT-2-4	9.1	white	tuff	Glass	Cc, Ha	Sm, Mi		D				
LT-2-5	11.8	white	mdst	Cc	Ab, Sm, Q	Ha, Mi		D		Fd	Sm, Q, I	
LT-2-6	13.9	white	tuff	Do	Q, Ab	Mi	OC-T, Sm	D(T)				
LT-2-7	15.3	white	tuff. ss	Ph		Q, Cc, Cl	Ha	Z				
LT-2-8	15.8	white	tuff. ss	Ph	Ha	Sm	Mi, Cl, Q	Z	Sm	Ph	I	
LT-2-9	22.5	pale yellow	mdst	Cl, Ph		Er, Sm, Mi	Q	Z	Cl, Ph		Sm, Er	Pa
LT-2-10	23.4	white	tuff	Cl	Ph	Er, Q		Z	Ph	Cl	Sm	Er
LT-2-11	24.6	pale yellow	tuff. ss	Ph, Cl	Q, Ab, Cc	Sm		Z				
LT-2-12	24.6	pale yellow & green	chert	Op		Q, Cl, Cc						
LT-2-13	17.4	white	tuff. ss	Cc, Q	Ph, Sm, Ab	Cl, Mi		D				
LT-2-14	18.0	pale yellow	tuff. ss	Q	Cc, Cl, Ph, Sm	Mi	Ab, Kf, Er	D				

(*continued*)

TABLE 1: BULK AND CLAY MINERAL COMPOSITION (CONTINUED)

Sample	Ht. in section (m)	Munsell color	Lithology*	Bulk Mineralogy†				Mineral facies§	Clay Mineralogy			
				Abundant	Common	Minor	Trace		Abundant	Common	Minor	Trace
LT-2-15	18.2	light gray	tuff. sltst	Cc	Sm, Q, Ab	Q, Mi	Ab, Kf	D				
LT-2-16	18.4	very pale brown	tuff. sltst	Do	Sm, Ab	Q, Cc, Mi		D(T)				
LT-2-17	18.9	white	tuff. sltst	Cc, Q, Ab	Sm	Mi, Do		D	Sm		I	Ph, Se, Chl
LT-2-18	19.4	white	tuff. sltst	Cc	Q, Ab	Sm, Mi		D				
LT-2-19	19.4	light gray	tuff. sltst	Q, Ab	Ha, Sm	Ph, Cl, Cc, Mi		D				
LT-2-20	19.8	white	tuff. ss	Cc, Do	Ha, Ab, Q, Sm	Cl, Mi		D(T)	Sm	Ph	Se, Cl	
LT-2-21	20.6	light gray	mdst	Sm, Se, Cc		Q, Mi, Pa	Fd	S				
LT-2-22	21.0	light gray	mdst	Se, Sm, Cc		Pa, Do, Q	Fd	S	Sm, Se	I		Pa
LT-2-23	21.6	light gray	mdst	Se, Cc, Sm		Pa, Q	Do	S	Sm, Se	I	Cl, Fd	Pa
LT-3-2	1.0	light gray	mdst	Akf, Mi	Cc, Sm		Gyp, Chl	K	I, Akf		Sm	
LT-3-4	2.8	light gray	mdst	Akf		Mi, Cc, Sr, Ha	Sm	K				
LT-3-6	6.8	light gray	mdst	Akf	Mi	Cc, Do, Sm	Sr	K	I, Akf		Sm	Ph
LT-3-9	8.8	light gray	mdst	Akf	Mi	Cc, Sm	Ha, Sr, Ma	K				
LT-3-11	11.7	white	tuff	Akf	Sr	Mi	Do, Sm	K				
LT-3-12	12.1	white	cherty tuff	Akf	OC-T	Mi, Cc, Sr	Do, Sm	K				
LT-3-13	11.3	pale yellow	cherty tuff	Akf	OC-T	Mi	Sm	K	Akf			OC-T
LT-3-14	12.7	light gray	mdst	Akf		Cc, Mi	Sm, Gyp	K				
LT-3-15	13.3	white	ss	Akf, Sr	Mi	Cc	Sm	K				
LT-3-16	14.6	gray and white	chert	Akf		Cc, Mi	Sm	K		I, Akf	Cl	Sm
LT-3-17	15.8	white	tuff. ss	Ab, Akf		Cc, Mi, An	Gyp, Ch, Ph, Ma	A				
LT-3-19	17.1	gray and white	tuff	Akf	Ha	Cc	Mi, Sm, Cl, Sr	K				

(*continued*)

TABLE 1: BULK AND CLAY MINERAL COMPOSITION (CONTINUED)

Sample	Ht. in section (m)	Munsell color	Lithology*	Bulk Mineralogy†				Mineral facies§	Clay Mineralogy			
				Abundant	Common	Minor	Trace		Abundant	Common	Minor	Trace
LT-3-20	17.5	very pale brown	mdst	Akf	Sm	Cc, Ab, Mi	Gyp, Cl, Ph	K	Akf, I		Sm	
LT-4-2	0.9	pink	mdst	Akf	Cc	Q, Ab, Mi, Sm	Er, Sr	K				
LT-4-3	1.5	light brownish gray	mdst	Akf, Cc		Q, Ha, Sm, Mi, Ab	Ph	K				
LT-4-4	1.6	white	tuff	Akf	Sm	Mi, OC-T, Cc	Q	K	Akf	I	Sm, Cc	
LT-4-6	1.9	pinkish white	mdst	Akf	Cc	Sm, Mi	Ab, Ph, Gyp	K				
LT-4-7	2.1	light gray	ss	Akf	Q, Cc	Ab, Mi, Sm	Er	K				
LT-4-8	2.6	light gray	mdst	Cc	Akf	Sm, Mi	Ab, Ph	K				
LT-4-10	3.7	light gray	mdst	Sm, Cc, Do		Fd, Mi, Ph		S				
LT-4-11	5.0	pale brown	mdst	Akf, Cc	Sm, Mi	An	Gyp	K				
LT-4-13	6.1	white	tuff	Sr, Ph, Akf	An	Cc	Mi, Sm, Er, Gyp	K				
LT-4-14	13.0	white	tuff	Ha	Akf	Sr, An, Mi, Cc	Sm, Ph	K				
LT-4B-1	0.7	light gray	sltst	Ab, Q, Cc		Ha, Mi, Sm	Cl	D				
LT-4B-2	1.5	very pale brown	tuff	Ph	An	Fd, Sm	Cl, Ha, Q	Z	Ph		Sm	Chl
LT-4B-3	2.0	light gray	sltst	Ab, Q	Cc, Kf	Mi, Sm	Gyp, Cl, Ph	D				
LT-4B-5	2.7	light gray	tuff	Ph	Q, An	Fd, Mi, Sm	Sr	Z				
LT-4B-6	2.8	light brownish gray	mdst	Cc	Sm	Fd, Q, Mi	Ph	S				
LT-4B-7	3.2	light gray	tuff. sltst	Q, Ab	Ph	Mi, Cc, Sm	Kf	D				
LT-4B-8	3.9	white	tuff	Ph, Ab	Q	Mi, Sm		Z	Sm	I, Ph		Chl
LT-4B-10	4.6	light gray	tuff. sltst	Q	Ab, Kf, Cc	Ph, Sm, Mi	Ha	D				

(*continued*)

TABLE 1: BULK AND CLAY MINERAL COMPOSITION (CONTINUED)

Sample	Ht. in section (m)	Munsell color	Lithology*	Bulk Mineralogy†				Mineral facies§	Clay Mineralogy			
				Abundant	Common	Minor	Trace		Abundant	Common	Minor	Trace
LT-4B-11	4.8	gray	mdst	Q, Sm, Cc		Fd, Ph, Mi	Ch, Sr	S				
LT-4B-12	5.3	light gray	tuff. ss						I	Sm, Cl, Ph		
LT-4B-14	6.9	pale yellow	ss	Ab, Q	Mi, Sm, Cc, Cl			D				
LT-4B-15	7.3	white	tuff. ss	Ph	Cc, Mi, Sr, Sm	Q, Cl		Z				
LT-4B-16	7.5	white	tuff	Ph	Q, Cc, Mi	Sm, Akf	Mo, Cl	Z				
LT-4B-17	7.9	white	tuff	Ph, Q	Fd	Cl, Mi		Z	Ph	I, Cl	Sm	
LT-4B-18	6.0	very pale brown	ss	Ab, Q	Cl, Mi	Cc, Gyp	Ph	D				
LT-4B-20	11.9	pale yellow	tuff. ss	Ab, Q	Mi, Sm, Cc	Ph		D				
LT-4B-21	14.4	white	tuff	Cc	Sm	Q, Mi	Cl	S				
LT-5-1	1.6	light gray	tuff. mdst	Sm, Do	Cc, Mi, Akf		Cl	S				
LT-5-3	5.5	light gray	mdst	Do, Akf	Ph, Cc, Sm	Mi, Ha		K				
LT-5-4	6.1	white	mdst						I, Akf		Ph, Sm, Do	
LT-5-5	7.1	light gray	tuff. mdst						I, Sm	Akf, Do	Ph	
LT-5-6	8.2	light gray	tuff. sltst	Akf	Cc, Mi, Ab, Sm	Ha	Sr	K	I	Sr, Akf	Sm, Chl	
LT-5-7	9.0	light gray	tuff. mdst						Sm	I, Do	Akf, Ph	
LT-5-8	10.0	white	tuff	Akf, Sr	Mi, Cc, Sm	Ha, Cl	Gyp	K	Sm, Sr		I, Akf	
LT-5-9	11.4	white	tuff. mdst						I	Akf	Sm, Sr	
LT-5-10A	12.0	light gray	mdst						Sm, I	Akf	Ph, Chl	
LT-5-10B	12.0	light gray	pseudomorph	Cc								
LT-5-12	14.2	light gray	mdst	Akf, Sm	Cc, Do	Sr, Mi, Ha		K				

(*continued*)

TABLE 1: BULK AND CLAY MINERAL COMPOSITION (CONTINUED)

Sample	Ht. in section (m)	Munsell color	Lithology*	Bulk Mineralogy†				Mineral facies§	Clay Mineralogy			
				Abundant	Common	Minor	Trace		Abundant	Common	Minor	Trace
LT-5-14	16.5	pale yellow	tuff. mdst	Akf		Cc, Mi, Ha, Sm	Gyp, Sr	K				
LT-6-2	1.8	white	tuff. sltst	Akf	Cc, Mi, Sm, Ab	Srl, Q	An	K				
LT-6-4	3.0	light gray	tuff. sltst						Akf, I		Sm	Do
LT-6-5	3.6	light gray	tuff	Akf	Mi	Srl, Ha, Sm, Cc	Cr	K	Akf	I	Sm, Sr	Chl
LT-6-8	5.7	light gray	mdst	Akf	Cc, Sm, Mi, Srl	Q		K				
LT-6-9	5.8	light greenish gray	tuff						Akf, OC-T	Er	I, Sm	
LT-6-10	6.3	very pale brown	ss	Akf	Mi, Cc, Srl	Sm		K				
LT-6-11	6.6	very pale brown	sltst						Akf, I	OC-T	Sm	Er, Chl
LT-6-14	8.9	very pale brown	mdst	Ab, Q	A?kf, Mi	Sm, Ha	Cl, An, Ph	A				
LT-6-15	9.3	light gray	ss						Akf, I, OC-T		Sm	Chl
LT-6-17	11.0	pale yellow	sltst	Ab, Q	A?kf, Mi, An	Cc, Ha, Sm	Cl	A				
LT-6-18	12.1	pale yellow	sltst						Akf, I	Sm		Chl
LT-6*-19	13.3	light gray	tuff. sltst	Q, Ab	Cc, Kf, Mi	Sm, Ha	Cl, An	?				
LT-6*-21	17.3	light olive gray	mdst		Cc, Kf, Sm, Er, Mi, Ph	Q, Ha	Cl	?				
LT-6*-22	19.3	light gray	tuff	Ph	Cl, Mi, Q, Cc	Sm		Z				
LT-6B-19	13.0	pale yellow	tuff. sltst	Q, Ab	Cc, Cl	Ph, Mi, Sm	Do, Ha	D				
LT-6B-20	14.4	light gray	sltst	Q, Ab	Cc	Sm, Mi	Do, Cl, Ha	D				
LT-6B-24	17.2	light gray	tuff. ss	Q, Ab	Kf, Sm	Cc, Cl, Gyp, An, Mi, Ha		D				

(*continued*)

TABLE 1: BULK AND CLAY MINERAL COMPOSITION (CONTINUED)

Sample	Ht. in section (m)	Munsell color	Lithology*	Bulk Mineralogy†				Mineral facies§	Clay Mineralogy			
				Abundant	Common	Minor	Trace		Abundant	Common	Minor	Trace
LT-6B-26	18.3	light gray	mdst	Ab, Cc, Q	Kf, Sm	Mi	Cl	D				
LT-6B-27	19.8	white	ss	Ab, Q	Cc, Kf	Sm, Mi, Ph	Gyp	D				
LT-6B-31	24.0	pale yellow	tuff	Cl, Ph, Ab	Q	Mi		Z				
LT-7-1	0.3	light brownish gray	tuff. mdst	Akf, Mi	Ch, Cc, Sm	Ph	Gyp, Ab	K				
LT-7-2	0.8	white	tuff	Akf, Mi, Sr	Cc, Sm	Ph, Er, Gyp	Ha	K	Akf	I	Sm	
LT-7-3	1.5	light gray	mdst	Akf, Mi	Cc, Sm	Gyp	Q, Ph, Er	K	I, Akf	Sm	I/S MLC	
LT-7-4	2.3	very pale brown	mdst	Mi, Akf	Sr, Sm, Cc	Cl	Ph, Q	K	I, Akf		Sm, Sr, I/S MLC	
LT-7-5	2.5	white	tuff	Sr, Akf		Mi, Q, Sm, Ph	Ha	K	Sr, Akf		I, Sm	
LT-7-6	3.3	light gray	tuff. ss	Akf, Mi	Sr, Cc	Cl	Sm	K	Sr, Akf	I	I/S MLC, Sm	
LT-7-7	4.5	light brownish gray	tuff. mdst	Akf, Cc	Gyp, Mi, Ph	Ab	Sr, Q, An, Sm, Er	K	Akf, Sm, I	Er	Gyp	
LT-7-8	5.8	white	tuff	Akf, Sr	Mi, Ph,	Ch, Cc, Sm	Ha	K	Sr, Akf	I	Ph, Sm	
LT-7-9	6.2	light gray	mdst	Akf	Mi, Sm, Cl	Cc, Q	Ab, Gyp, Ha	K	I	Sm, Akf	Cl, Ph	
LT-7-10	6.9	white	tuff	Akf, Sr	Mi, Cl, Ph	An, Sm, Gyp	Cc, Ha	K	Akf	I, Sr	Cl	
LT-7-11	8.1	very pale brown	tuff. mdst	Akf, Mi	Sr, Sm	Ph, Cl	Ha, Q, Er	K	I, Akf	Sr	Sm, Ch, Er	
LT-7-12	8.4	white	tuff. sltst	Akf	Sr, Mi, Sm	Ch, Cl	Cc	K	Akf, Sr	I, Cl	Sm	
LT-7-13	9.6	white	tuff. ss	Ab, Ch, Akf	An, Sr, Er	Cc, Ph, Mi	Gyp, Ha	A	Akf	I, Sr	Sm, Er, Cc	
LT-7-14	7.7	white	tuff. mdst	Mi, Sr	Akf, Ab, An, Ph	Er, Cc	Sm	K				
LT-7-15	8.7	white	tuff. ss	Sr, Akf	Mi, Ch	Mi, Ph, Sm, Ch, Er, Cc	Ph, Q, Sm	K	Sr, Akf	I	Er, Ch	

(*continued*)

TABLE 1: BULK AND CLAY MINERAL COMPOSITION (CONTINUED)

Sample	Ht. in section (m)	Munsell color	Lithology*	Bulk Mineralogy†				Mineral facies§	Clay Mineralogy			
				Abundant	Common	Minor	Trace		Abundant	Common	Minor	Trace
LT-7-16	9.1	light gray	tuff. mdst	Akf, Sm, Mi	Cc, Ab, Sr	Ph	Gyp, Ch, Cl	K	Akf, I, Sm	Ph	Er, Cc, Ha, Sr, Cl	
LT-7-17	9.3	white	tuff. ss	Akf, Ab	Mi, An	Ph, Cc, Gyp, Sm	Ha, Sr	K	Akf, I		Er, Sr, Sm	
LT-7-19	10.4	white	tuff. ss	Akf, Sr	Ab, Mi	Ph, Cl, An, Cc, Sm	Ha	K	Akf	Er, I	Sr, Sm	
LT-7-20	11.3	light gray	cherty tuff	Akf, Tri, Mi	Sr	Gyp, Sm	Cc, Er	K		Akf, I, Sr	Er	
LT-7-21	12.0	gray	cherty ss	Akf, OC-T	Sr, Cc, An	Mi, Sm, Ch, Ph	Ha	K	Akf	I		
LT-7-22	13.9	white	tuff. mdst	Akf, Mi	Er	Cl, Ph, Cc, Gyp	Ha, Sm	K		Akf, I	Sm, Cl, Cc	
LT-7-23	14.7	light gray	mdst	Mi, Sm	A?Kf,	Cc, Ab, Ch, Gyp	Q, Ph, Ha	S	I, Akf	Cc	Se, Sm	
LT-7-24	16.5	white	tuff	Akf	Mi, Ab	Sm, Cl, Ph, An	Gyp, Cc	K	Sm, I		Cl, Akf	
LT-7-25	18.2	light gray	mdst	Mi, Akf	Sm	Cl, Ph, Cc, Gyp, Ch		K	Akf	I, Sm	Cc, An, Ch, Er	
LT-7-28	22.7	white	tuff. mdst	Ab	Akf, Sm, Mi, An, Cl	Cc	Ha	A	Akf, I	An	Cc, Sm	
LT-7-30	26.1	light olive gray	mdst	Sm, Mi	Kf, Ab	Ch, Cc, Q	Gyp	S	Sm	I	Cc, Cl, Fd	
LT-7-31	26.2	white	tuff	Ph, Cl		Akf, Q, Mi	Sm, Ha	Z	Ph	Akf, I		
LT-7-32	27.2	light gray	cherty tuff	OC-T, Akf	Cl, Ch	Mi, Sm	Cc	K?	Akf		I, Sr	
LT-7-33	30.5	pale yellow	tuff. ss	Akf, Ab	Mi	Ph	Sm, Q, Cc, Gyp	K				

*Lithological abbreviations: ss—sandstone; sltst—siltstone; mdst—mudstone; tuff—tuffaceous.

†Mineralogical abbreviations: Ab—albite; Akf—authigenic potassium feldspar; An—analcime; Cc—calcite; Ch—chabazite; Chl—chlorite; Cl—clinoptilolite; Do—Dolomite; Er—erionite; Fd—undifferentiated feldspars; Gyp—gypsum; Ha—halite; I—illite; I/S MLC—illite-smectite mixed-layered clay; Kf—undifferentiated potassium feldspar; Mi—undifferentiated mica; Mo—mordenite; OC-T, Opal C-T—Pa, palygorskite; Ph—phillipsite; Q—quartz; Se—sepiolite; Sm—smectite; Sr—searlesite; Tri—tridymite.

§Mineral facies abbreviations (see Table 2): D—detrital; S—smectite-carbonate; Z—zeolite; K—authigenic potassium feldspar; A—authigenic albite; D(T) — detrital with dolomite from lake transgression.

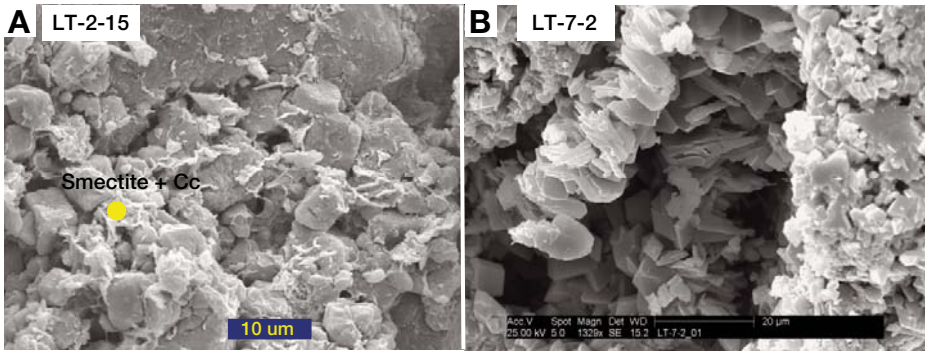

Figure 5. (A) Scanning electron micrographs illustrating detrital grains of quartz and feldspar with interstitial clays bridging between grains; sample LT-2-15. (B) Scanning electron micrographs of authigenic potassium feldspar and searlesite (presumably after phillipsite or clinoptilolite) lining a shard cavity in a tuff; sample LT-7-2. Yellow dot indicates location of qualitative energy dispersive X-ray analyses that assist with mineral identification.

Authigenic Nonsilicate Minerals

Calcite, dolomite, gypsum, and halite are present in variable quantities in many or most samples. Calcite is present in most samples, but is only a major constituent in the tufa deposits, some alluvial sands, and green claystones. Dolomite is present in a few samples from the lacustrine-margin facies, but is most common in green claystones. Gypsum and halite are present in trace quantities in samples from all facies.

DISCUSSION

Tecopa Basin Depositional Environments

The clastic sediment in the Lake Tecopa beds is interpreted to have been derived primarily from four sources: the ancestral Amargosa River, locally derived epiclastic sediment, eolian silt and sand, and volcanic ash. Sediment from the Amargosa River aggraded fluvial deposits, built deltas, and contributed to lacustrine margin sediments (e.g., beaches, bars). The locally derived epiclastic sediment was deposited as debris flows and sheet floods on fans, alluvial flats, and mudflats, and contributed to lacustrine-margin sedimentation. Much of the fine sand and silt in the subaerial and lacustrine-margin deposits is interpreted to be eolian in origin. The importance of eolian processes may also contribute to the absence of well-developed soil horizons, as observed by Morrison (1999). Periodic pulses of eolian aggradation would have limited soil development on the landscape, resulting in stacks of weakly developed paleosols, such as those observed in the lower part of section LT-2. Volcanic ash originated from several eruptive centers in western North America (Sarna-Wojcicki et al., 1987), fell on the landscape in the Tecopa drainage basin, and was washed and blown by wind into the lake basin. The main sediments within the lacustrine facies are mud and ash, which likely settled from suspension from either hyperpycnal flows or eolian fallout.

Chemical sedimentation occurred in the form of calcite tufa at and near springs and as authigenic minerals precipitating in lacustrine sandstone, siltstone, and mudstone. The tufa deposits are aligned along structural features and appear to have been formed during and after Lake Tecopa sedimentation (Nelson et al., 2001). Saline, alkaline lake-water chemistry is indicated by gaylussite molds and calcite pseudomorphs after trona in mudstone, and authigenic silicate alteration patterns in mudstone and tuff (Sheppard and Gude, 1968; Starkey and Blackmon, 1979; Larsen, 1997). The extensive magadiite-type chert in the mudflat and shallow-lacustrine deposits is also consistent with this interpretation.

A modern sedimentary analog to ancient Lake Tecopa is Lake Bogoria in the Kenya rift valley, East Africa. Lake Bogoria is a perennial saline, alkaline lake with a single major feeder stream and delta (Sandai River and its delta), several enclosing alluvial fans, and vegetated (marsh) margins (Renaut and Tiercelin, 1994). The surface area of Lake Bogoria is approximately an order of magnitude smaller than that of Lake Tecopa at its highest late Pleistocene level (~235 km^2; Morrison, 1991), but might be comparable to Lake Tecopa during late Pliocene or middle Pleistocene time. Water depths in Lake Bogoria were as much as 11.5 m during historic highstands. Lacustrine-margin sedimentation is dominated by interbedded sands, silts, and muds, commonly bearing root traces. Deeper-water sediments are dominantly muds with dispersed gaylussite, nahcolite, and trona crystals, and rare centimeter-thick intervals of trona and associated evaporites. During the low, early Pleistocene lake levels (1.6–0.9 Ma) of Lake Tecopa, the lake may have appeared similar to a slightly wetter version of modern-day Lake Magadi, East Africa. Lake Magadi is a saline, alkaline lake with extensive enclosing sandflats and mudflats, in which magadiite precipitates in the lacustrine-margin deposits but is replaced on the mudflats by flaggy cherts, typically containing gaylussite or trona molds (Eugster, 1980). In contrast to the east African lakes, eolian depositional processes appear to have been much more important at Tecopa.

Lake Level through Time

The lake-level history inferred from this work (Fig. 8) generally follows the results of other investigators (Morrison, 1991, 1999; Larson et al., 1991), but some differences are noted. The basin-fill history recorded in the sections illustrated in Plate 1 extends from some time prior to the 2.02 Ma Huckleberry Ridge ash to some time after the 0.665 Ma Lava Creek B ash. Pre–Huckleberry Ridge depositional conditions are represented by basin-center exposures of strata reflecting relatively shallow to deeper perennial lake environments. Lake level during this time is difficult to reconstruct due to a lack of correlative basin-margin exposure; however, a perennial lake of varying extent is inferred based on the extent of green mudstone facies (Plate 1) analogous to perennial lake facies within younger deposits. This contrasts with the interpretation of Morrison (1991, 1999) that only playa and shallow lake deposits are represented below the Huckleberry Ridge ash.

Lake level lowered rapidly during and following emplacement of the Huckleberry Ridge ash. Much of the central basin floor appears to have been an extensive mudflat, subject to alternating wetting and drying conditions. Lacustrine deposits are present at section LT-5, but contain calcite pseudomorphs after trona and cherty alteration, suggesting more concentrated brines and lower lake levels in the basin center. This episode of dramatically lower lake level roughly corresponds to the 1.6–0.9 Ma interval of "dry lake" conditions identified by Larson et al. (1991) and discussed by Morrison (1999).

Lake level appears to have risen from ca. 1.0 Ma to some time after eruption of the 0.76 Ma Bishop ash. Two pronounced peaks in lake level are shown in the post–Bishop ash strata in Plate 1: one immediately following emplacement of the Bishop ash and the other immediately prior to the 0.665 Ma Lava Creek B ash. Judging from the extent of lacustrine incursion at section LT-1 and other locations around the margin of the basin, the highstand immediately following the Bishop ash appears

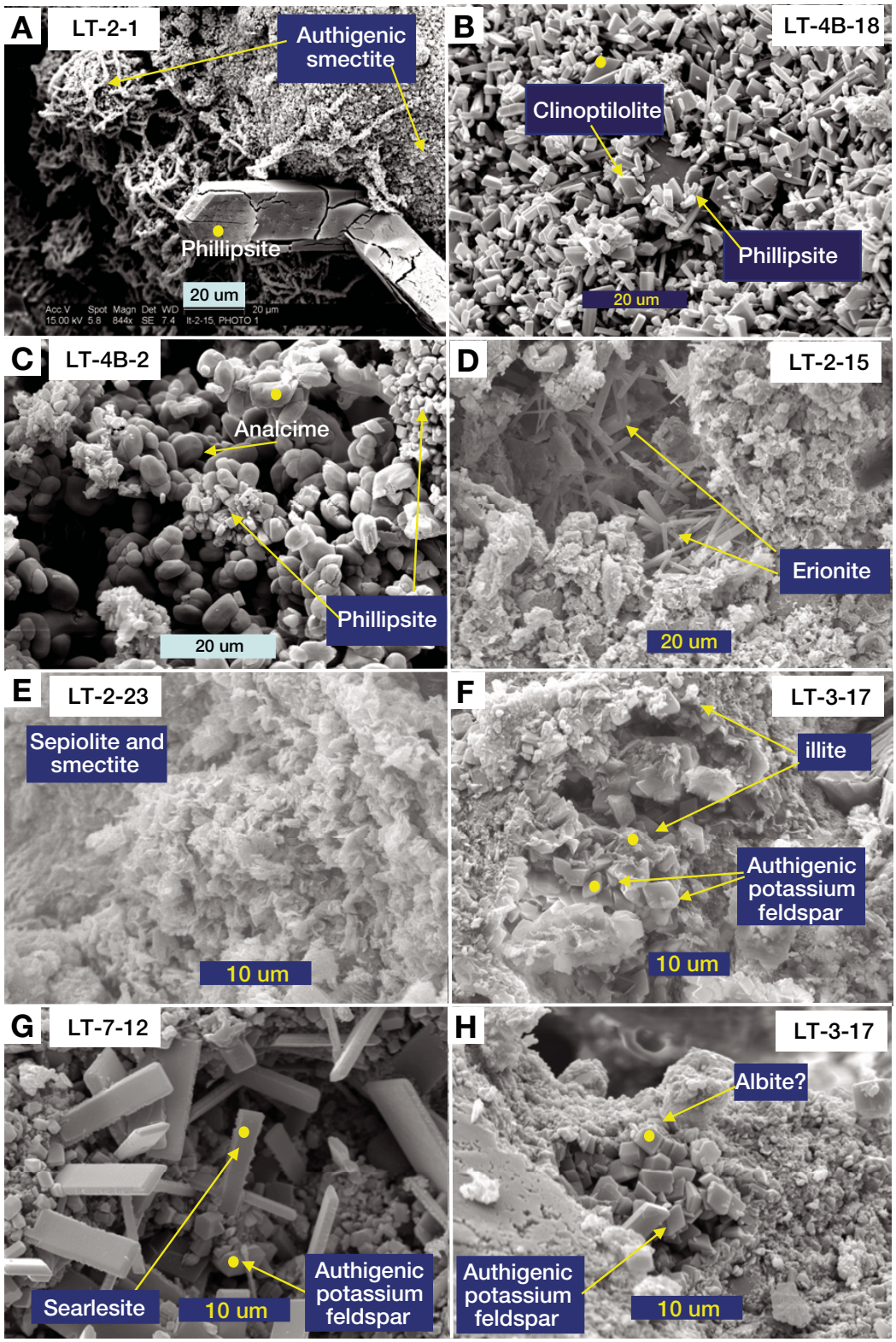

Figure 6. Scanning electron micrographs of diagenetic minerals. Yellow dots indicate locations of qualitative energy dispersive X-ray analyses (EDX) that assist with mineral identification. (A) Grain-coating matte of smectite with prisms of phillipsite and vermicular smectite in pore space; sample LT-2-1, tuffaceous siltstone. (B) Grain-coating of intergrown clinoptilolite, phillipsite, and erionite; sample LT-4B-18, sandstone. (C) Euhedral analcime replacing phillipsite; sample LT-4B-2, tuff. (D) Erionite replacing glass shard within clay and detrital mineral matrix; sample LT-2-15, tuffaceous siltstone. (E) Fibrous sepiolite and cornflake trioctahedral smectite; sample LT-2-23, mudstone. (F) Authigenic illite lining pores partially filled with authigenic potassium feldspar; sample LT-3-17, tuffaceous sandstone. (G) Pore lined with fine authigenic potassium feldspar and 10–20-μm-long laths of searlesite; sample LT-7-12, tuffaceous siltstone. (H) Pore lined with authigenic albite(?) and potassium feldspar; sample LT-3-17, tuffaceous sandstone.

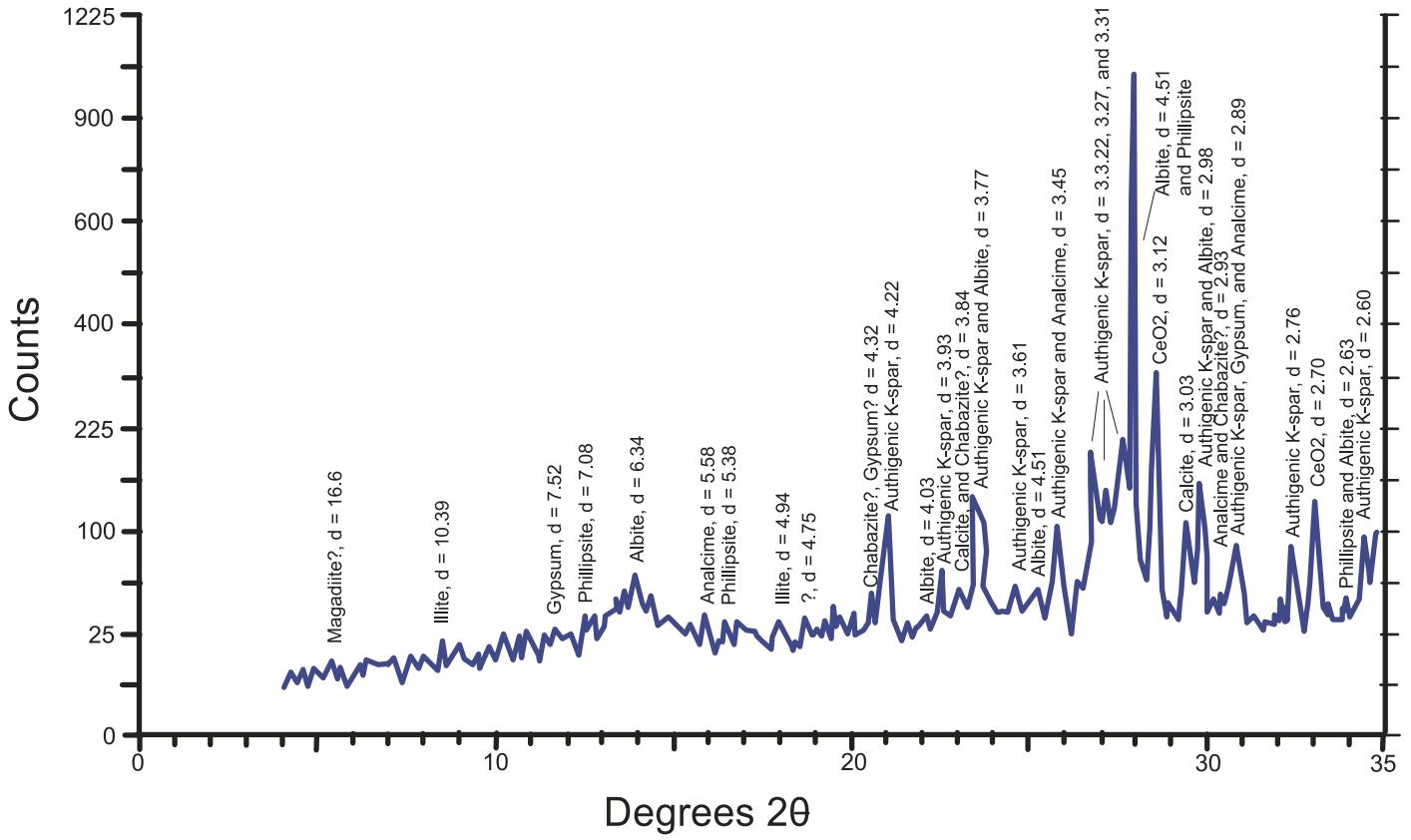

Figure 7. X-ray diffraction pattern of sample LT-3-17 illustrating diffraction maxima for authigenic albite and associated authigenic minerals. D-spacings are given in angstroms.

to have been the higher of the two. Lake levels fell and rose several times after emplacement of the Lava Creek B ash, but the record is confined to a few high-level sections and wave-cut terraces around the basin margin. Late Pleistocene wave-cut terraces around the basin margin argue for a late highstand prior to the ultimate demise of Lake Tecopa, ca. 0.2 Ma (Morrison, 1991; Anderson et al., 1994).

The lake-level history of Lake Tecopa generally follows regional trends during late Pliocene through middle Pleistocene time. The earliest deposits reflect intermediate lake levels from ca. 2.4 to 2.0 Ma (Huckleberry Ridge ash), consistent with inference from Pliocene deposits in the Amargosa Desert (Hay et al., 1986). This contrasts with the Searles Lake record (Morrison, 1999), which shows relatively low lake levels at that time. Lake Tecopa underwent a period of pronounced desiccation from ca. 2.0 Ma to prior to ca. 1.0 Ma (Glass Mountain G ash), which generally corresponds to a period of intermediate to low lake levels in the Owens Valley River system (Jannik et al., 1991). Lake levels rebounded to intermediate levels ca. 1.0 Ma, but rose and then fell abruptly prior to Bishop ash eruption at 0.76 Ma. The short-lived rise in lake level prior to the Bishop ash may correspond to a similar event in Searles Lake (Jannik et al., 1991); however, no correlative decline in lake level is reported from other lakes in the region. Two highstands in Lake Tecopa between the Bishop and Lava Creek B ashes appear to correlate with similar highstands in Searles Lake (Jannik et al., 1991) and Lake Bonneville (Morrison, 1999). The post–Lava Creek B section shows evidence for at least two subsequent highstands; however, the lack of well-preserved interbedded ashes limits correlation to regional events.

Authigenic Mineralogy

Evidence from SEM and XRD analysis suggests that most of the clay minerals in the lacustrine facies and even some in the subaerial facies are authigenic in origin. Starkey and Blackmon (1979) interpreted most clay minerals in lacustrine mudstones as being dominantly detrital; however, the dominance of trioctahedral smectite, homogeneity of clay mineral compositions in the lacustrine mudstones, and SEM textures observed in this work suggest an authigenic origin. Trioctahedral smectite + sepiolite + carbonate assemblages are well documented in Pliocene–Pleistocene spring and shallow lake deposits in the Amargosa Desert and are interpreted to have precipitated from pH-neutral, fresh spring waters (Khoury et al., 1982). Clay mineral authigenesis in lacustrine mudstones near spring deposits along the northern margin of Lake Tecopa (sections LT-1 and LT-2), where sepiolite and palygorskite are observed with trioctahedral smectite, likely precipitated in a similar chemical setting. However, trioctahedral smectite also formed within the lake as a result of reaction of detrital clay minerals with Mg-bearing alkaline and mildly saline pore fluids, similar to conditions described by Banfield et al. (1991) at Lake Abert, Oregon (Jones and Weir, 1983), and Deocampo et al. (2002) and Hover and Ashley (2003) at Olduvai Gorge, Tanzania. SEM evidence (Fig. 6) suggests that smectite authigenesis also occurred during the early phases of hydration and solution of volcanic glass in tuffaceous strata (e.g., Taylor and Surdam, 1981); however, this likely resulted in more aluminous, dioctahedral clay compositions. Illite tends to dominate in the authigenic

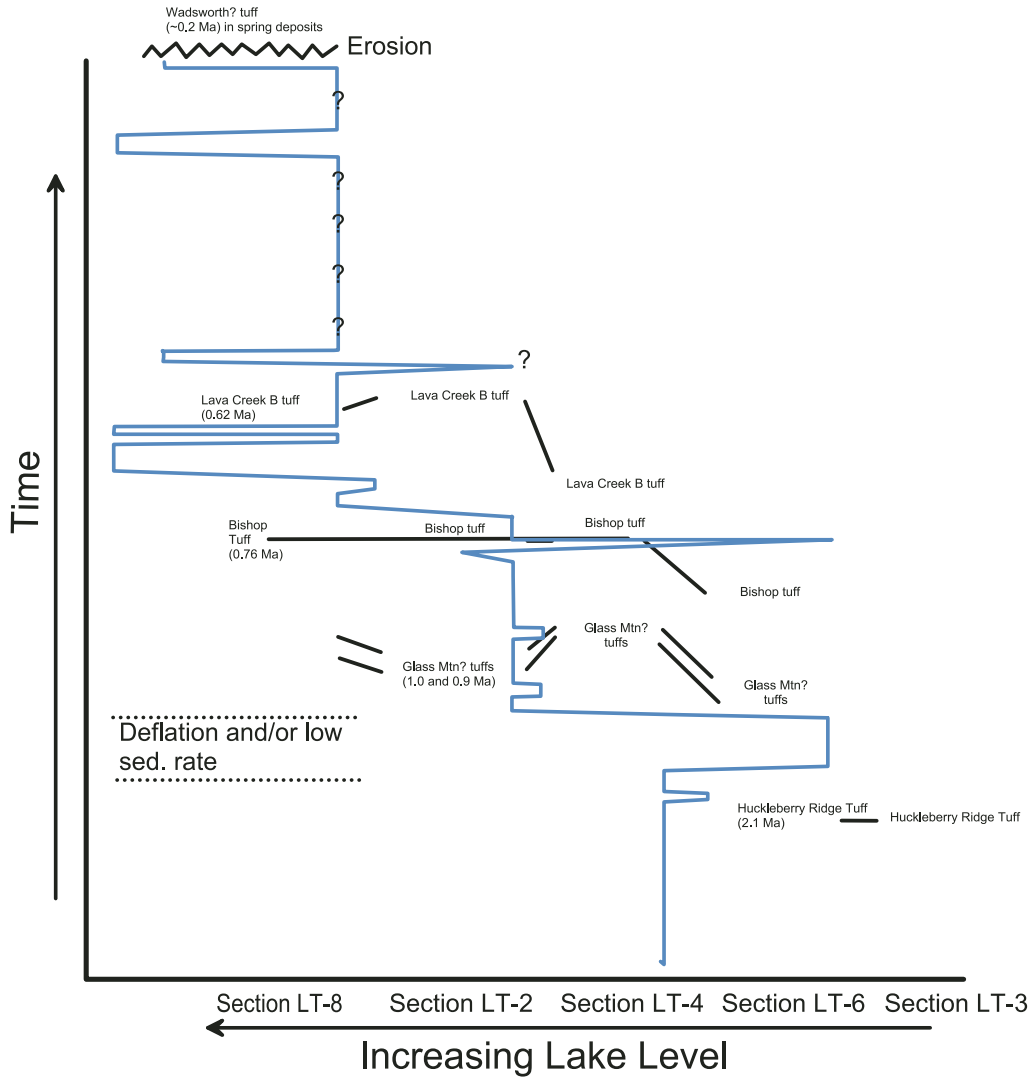

Figure 8. Schematic lake level variation through time for Lake Tecopa. Sed.—sedimentation.

potassium feldspar and albite mineral facies and clearly shows authigenic mineral textures (Fig. 6). Unlike similar occurrences of illite at Olduvai Gorge (Hay and Kyser, 2001), little or no mixed layering with smectite is observed. Formation of illite is favored by a high K/Mg ratio and salinity, and likely results from neoformation from the most saline pore-fluid compositions (Hover and Ashley, 2003).

Reaction of volcanic glass and other labile silicate materials with increasingly saline and alkaline waters have been shown through field observations (Hay, 1966; Surdam and Eugster, 1976; Taylor and Surdam, 1981) and laboratory investigations (Wirsching, 1976; Hawkins et al., 1978; Hawkins, 1981) to result in precipitation of a suite of authigenic clay minerals, zeolites, potassium feldspar, and silica minerals. Alkali zeolites line pores and partially replace shards and pumice, and include the most commonly observed alkali zeolites in saline, alkaline lake deposits (Chipera and Apps, 2001), i.e., phillipsite, clinoptilolite, erionite, chabazite, and analcime (Fig. 6). The silica-rich alkali zeolites (excluding analcime) are favored by dissolved silica contents greater than that of quartz saturation and lower dissolved sodium contents; however, the actual mineral species that dominates appears most sensitive to pH (silica and aluminum solubility) and cation ratios (Surdam and Eugster, 1976; Surdam, 1977; Bowers and Burns, 1990; Chipera and Apps, 2001). The commonly observed assemblage of phillipsite, clinoptilolite, and erionite in Lake Tecopa sediments suggests that subtle changes in pore-fluid conditions may have controlled the presence of these mineral species. Chabazite is more limited to basin-central locations and may reflect later stage equilibration with potassium feldspar or analcime, consistent with geochemical modeling results of Chipera and Apps (2001). Analcime is not abundant in the Tecopa beds, but is found in presumed reaction relationship with phillipsite (Fig. 6C) and in minor to common amounts in association with authigenic potassium feldspar and albite in the basin-central facies. Authigenic potassium feldspar and accompanying illite are ubiquitous in the central part of the Tecopa basin and are interpreted to reflect reaction with the most concentrated pore waters, similar to observations in other saline, alkaline lake environments (Surdam and Sheppard, 1978; Hay and Kyser, 2001).

Whereas the presence of the zeolites and authigenic potassium feldspar is well documented in other late Cenozoic saline, alkaline lake deposits (Hay, 1966; Sheppard and Gude, 1968; Surdam and Sheppard, 1978), the presence of authigenic albite is not as well documented in similar and older deposits (Surdam and Parker, 1972; Turner and Fishman, 1991). Its presence in the mudflat and shallow lacustrine facies may be related to analcime, possibly

formed in part due to exposure (e.g., Remy and Ferrell, 1989; Renaut, 1993), reacting with silica-bearing waters during desiccation:

$$NaAlSi_2O_6 + H_4SiO_4 = NaAlSi_3O_8 + 2\ H_2O. \quad (1)$$
(analcime) (albite)

Alternatively, it may form in association with destabilization of silica-rich alkali zeolites during an Ostwald reaction step (Chipera and Apps, 2001), where:

$$\text{Na-zeolite} + \text{opal C-T} = \text{albite} + \text{quartz} + H_2O. \quad (2)$$

The common association of quartz with albite (Table 1) suggests that reaction 2 may be more important in some cases.

The timing of authigenesis is difficult to constrain based on the available data, but evidence suggests that chemical reactions occurred during early diagenesis. The fact that alteration of individual beds resulted in sharp authigenic boundaries corresponding to sedimentological indicators (and not necessarily sediment composition) of change in lake level suggests that authigenesis occurred prior to diffusion of saline alkaline solutions across bedding boundaries. Sediment composition plays an important role in that abundant volcanic glass tends to hydrolyze rapidly and drive solutions toward more saline and alkaline compositions (Hay, 1966; Mariner and Surdam, 1970). Hydrology also plays an important role in that flow-through systems (i.e., hydrologically open) tend to maintain fresher, mildly alkaline solution compositions that result in precipitation of smectite and alkali zeolite minerals (Sheppard and Hay, 2001). Hydrologically closed systems, such as closed lakes, tend toward more evaporatively concentrated, alkaline waters, which result in precipitation of alkali zeolites and authigenic feldspars (Surdam and Sheppard, 1978). Given that the sediment composition and hydrologic conditions vary within the Tecopa basin, the authigenic mineralogy and mineral distributions are expected to be somewhat complex; however, the dominance of one or more factors may primarily determine the authigenic mineral composition within various parts of the basin.

Mineralogical and Sedimentary Facies Relationships

Mineralogical facies have been designated to facilitate comparison of mineral distributions with sedimentary facies patterns and are described in Table 2. The detrital mineral facies is dominated by nonauthigenic minerals. The detrital facies with transgressive overprint is the same as the detrital facies except that diagenetic calcite and dolomite are major mineral phases. The smectite and carbonate, zeolite, authigenic potassium feldspar, and authigenic albite facies are composed mainly of authigenic minerals.

The mineral facies distributions are overlain on the stratigraphic distribution of depositional environments along the axis of the basin in Plate 2 and transverse to the basin axis in Figures 9 and 10. Mineral facies distributions follow depositional environment patterns to varying degrees, but seem to correlate best in the basin-margin sections such as LT-1 and LT-2 (Plate 2), LT-6B (Fig. 9), and LT-4B (Fig. 10). Along the axis of the central basin, the authigenic potassium feldspar mineral facies dominates, although the authigenic albite mineral facies seems to correlate well with the latter part of the lowstand following the Huckleberry Ridge ash (Plate 2) and the smectite and carbonate mineral facies corresponds with several relatively deep perennial-lake events (Plate 2 and Fig. 9).

Sediment composition, especially the content of volcanic ash, appears to locally influence authigenesis within individual beds. As noted by Sheppard and Gude (1968) and Starkey and Blackmon (1979), ash-rich beds tend to be altered to various zeolites even in nonlacustrine and lacustrine-margin environments. This relationship is particularly well demonstrated in the lower 8 m of section LT-4B (Fig. 10), where five of six ash beds are altered to phillipsite regardless of whether they occur in alluvial-flat, lacustrine-margin, or shallow lacustrine facies. On a microscopic scale, volcanic shards have been dissolved and partially lined with phillipsite, erionite, or clinoptilolite, even in pedogenic mudstones. Such observations argue that pore-water compositions in nonlacustrine facies around the basin margin vary on a centimeter scale, probably reflecting frequency and degree of water saturation, saturation-dependent changes in hydraulic conductivity, and periodicity of fresh-water flushing.

Mineralogy and Lake Level through Time

Mineralogical facies are variably affected by changes in lake level and associated hydrologic impacts. In basin-margin sections, mineralogical facies commonly follow sedimentological indicators of lake level. For example, in sections LT-2 and LT-4B zeolitic shallow-lacustrine intervals alternate with detrital-dominated alluvial-flat and lacustrine-margin intervals or trioctahedral smectite and carbonate-bearing deeper lacustrine intervals. In some cases, such as at section LT-2 (13–15 m and 18–19 m in Plate 2), the transgression of lake water over lake-margin calcareous paleosols and sediments apparently drove precipitation of dolomite in the marginal facies, presumably by reaction of magnesium-bearing lake water with soil- or groundwater-formed calcite. In sections off the basin center, such as sections LT-4 and LT-7, the deeper lake facies are commonly mineralogically distinct from the shallow water or mudflat facies. However, at sections LT-3, LT-5, and LT-6, such variations are masked by a diagenetic overprint, likely due to progressive long-term lowering of lake level and alteration during the early Pleistocene.

The effects of long-term lake level change on mineralogy are most readily seen in the successive mineralogical changes observed in the pre- and post-Huckleberry Ridge ash intervals at sections LT-3, LT-5, and LT-7 (Plate 2 and

TABLE 2. MINERALOGICAL FACIES COMPOSITION OF SAMPLES

Mineral facies	Major and minor mineral constituents*
Detrital	Quartz + albite + potassium feldspar + *smectite* (trioctahedral and dioctahedral) + illite + minor *calcite, clinoptilolite*, *phillipsite,* chlorite*,* and salts
Detrital with transgressive overprint	*Calcite* + *Dolomite* + Quartz + albite + potassium feldspar + *smectite* (trioctahedral and dioctahedral) + illite + minor *clinoptilolite*, *phillipsite,* chlorite*,* and salts
Smectite + carbonate	*Trioctahedral smectite* + *calcite* + *dolomite* + minor *clinoptilolite*, *phillipsite*, *sepiolite*, feldspars, quartz, and salts
Zeolite	*Phillipsite* + *clinoptilolite* + *erionite* + quartz + albite + *analcime* + minor other feldspars, *calcite*, *smectite*, illite, *searlesite*, and salts
Authigenic potassium feldspar	*Potassium feldspar* + *illite* + *searlesite* + *chabazite* + *analcime* + *albite* + minor *calcite*, *opal C-T*, *trioctahedral smectite*, *other zeolites*, and salts
Authigenic albite	*Albite* + *potassium feldspar* + *illite* + *analcime* + *searlesite* + *chabazite* + minor *calcite*, *trioctahedral smectite*, *other zeolites*, and salts

*Minerals in italics are interpreted to be authigenic, all others are likely detrital or a result of modern weathering.

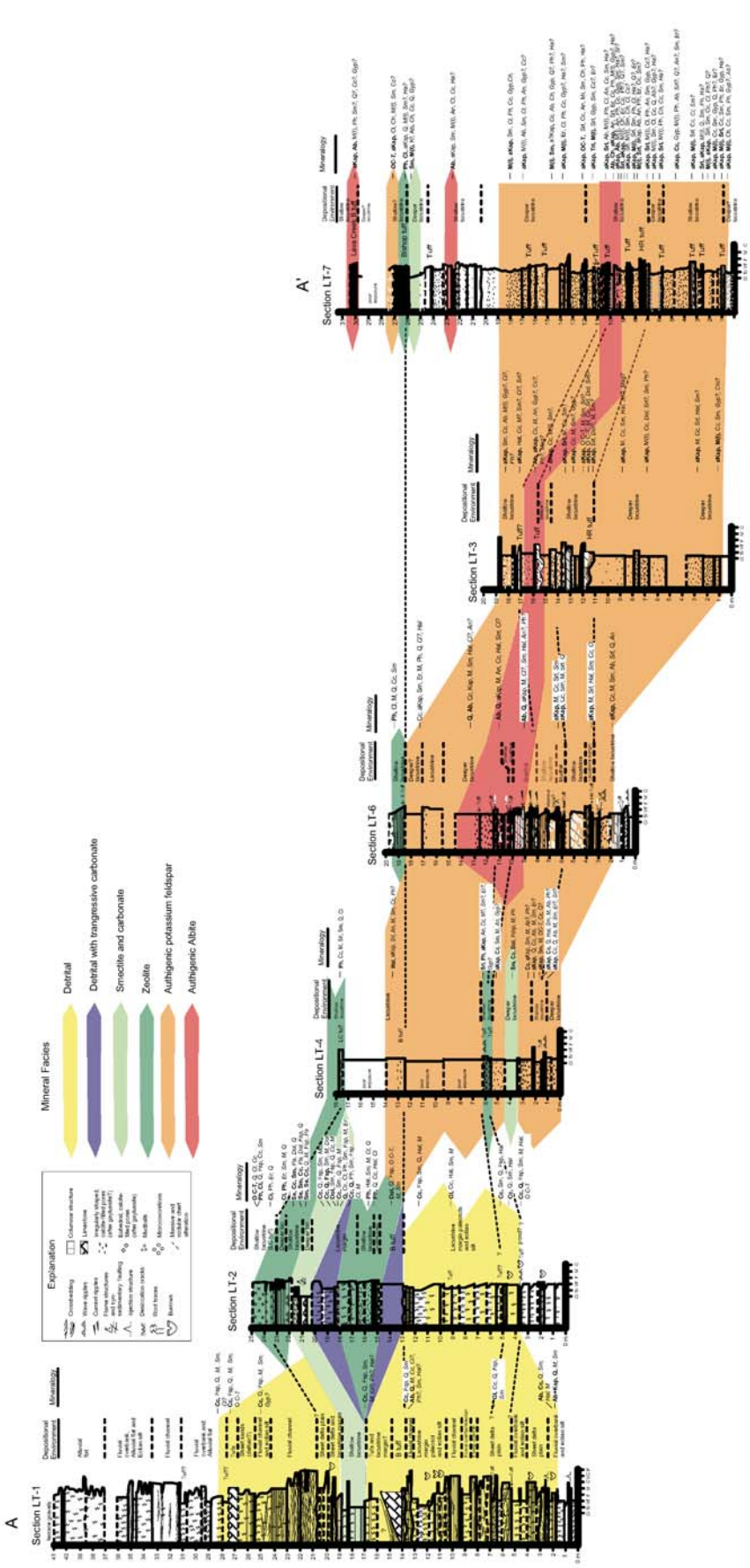

Plate 2. Color overlay of mineralogical facies along cross-section A-A' including sections LT-7, LT-3, LT-6, LT-4, LT-2, and LT-1. Mineralogical abbreviations: Ab—albite; Aksp—authigenic potassium feldspar; An—analcime; Cc—calcite; Ch—chabazite; Chl—chlorite; Cl—clinoptilolite; Dol—dolomite; Er—erionite; Fsp—undifferentiated feldspars; Gl—glass; Gyp—gypsum; Hal—halite; I—illite; Ksp—undifferentiated potassium feldspar; Mag—magadiite; M—undifferentiated mica; M(I)—illite; Mic—microcline; Mo—mordenite; OC-T—opal C-T; Pa—palygorskite; Ph—phillipsite; Q—quartz; Se—sepiolite; Sm—smectite; Srl—searlesite; Tri—tridymite. Mineral abundances: major—bold font; common—normal font; minor—italic font; trace—italic font with question mark. See Plate 1 for grain size abbreviations. If you are viewing the PDF of this paper or reading it offline, please visit http://dx.doi.org/10.1130/GES00152.SP2 (Plate 2) or the full-text article on www.gsajournals.org to view Plate 2.

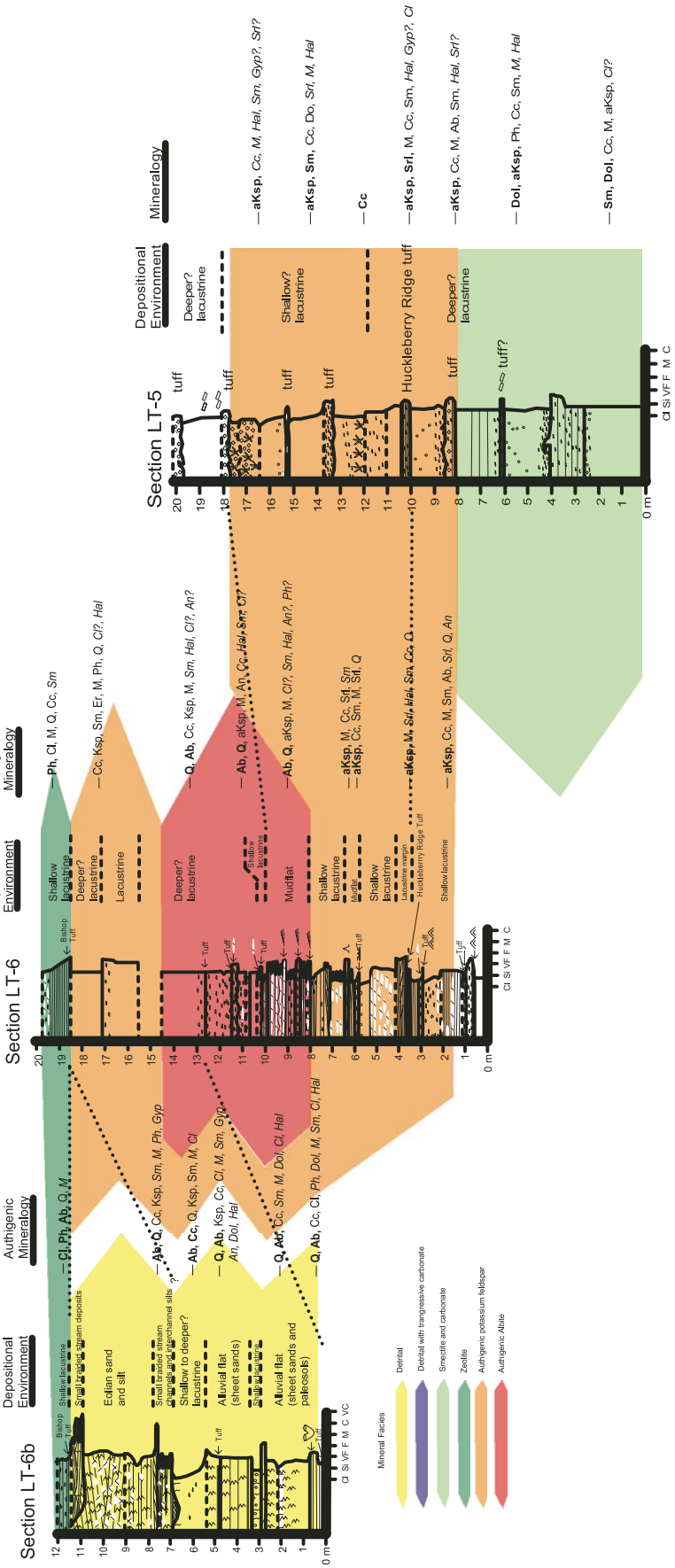

Figure 9. Color overlay of mineralogical facies along cross-section B-B' including sections LT-6B, LT-6, and LT-5. See Plate 2 caption for mineral abbreviations. See Fig. 3 for grain size abbreviations.

Fig. 9). Deeper lacustrine facies with remnant smectite and carbonate mineralogy give way upward to authigenic potassium feldspar and illite mineralogy in shallow lacustrine facies and ultimately to authigenic albite mineralogy in mudflat and shallow lacustrine facies. The albite facies correlates well with a period of trona formation (calcite pseudomorphs preserved) at section LT-5, which suggests that these mineral precipitates formed from a concentrated brine. The predominance of the authigenic feldspar (both potassium feldspar and albite) and illite minerals throughout the basin-center sections suggests that the basin-center brine migrated vertically and altered the initial authigenic mineralogy of the basin-center facies through time. This diagenetic overprint was less complete in sections LT-7 and LT-4, which are off the basin center. The timing of the diagenetic overprint was likely soon after deposition. A K-Ar date on authigenic feldspar from a bed a few meters below the Huckleberry Ridge ash (2.01 Ma) gave an age statistically indistinguishable from the ash (Stephen Nelson, 1999, personal commun.), suggesting that alteration occurred within a matter of tens of thousands of years, consistent with observations at Teels Marsh, Nevada (Taylor and Surdam, 1981).

Implications for Closed-Basin Hydrology

The authigenic mineral patterns observed in the Lake Tecopa beds conceptually match with its closed-basin hydrology and provide further information about paleohydrologic conditions. During late Pliocene and early to middle Pleistocene time, Lake Tecopa was a closed hydrologic basin with little or no groundwater drainage. The timing of surface-water overflow at the south end of the basin is debated (Larsen et al., 2003; Morrison, 1999), but likely became integrated with Death Valley via the Amargosa River after ca. 200 ka (Morrison, 1999). Thus, during Pliocene through middle Pleistocene time, surface water and groundwater discharged in the basin were lost solely by evaporation. Reaction of generally alkaline groundwater in the region (Claassen, 1985; Thomas et al., 1996) with copious amounts of volcanic ash and evaporation served to drive lake-water composition toward a saline, alkaline brine (e.g., Eugster and Hardie, 1978).

Duffy and Al-Hassan (1988) explored groundwater-flow patterns in closed hydrologic basins using empirical data and computer simulations. Two key characteristics appear to control groundwater flow patterns: the relief of surrounding mountains and the Rayleigh number (R_a) of the brine. In basins with relatively high topographic relief and high upland recharge, the resulting R_a is low and free convection of a

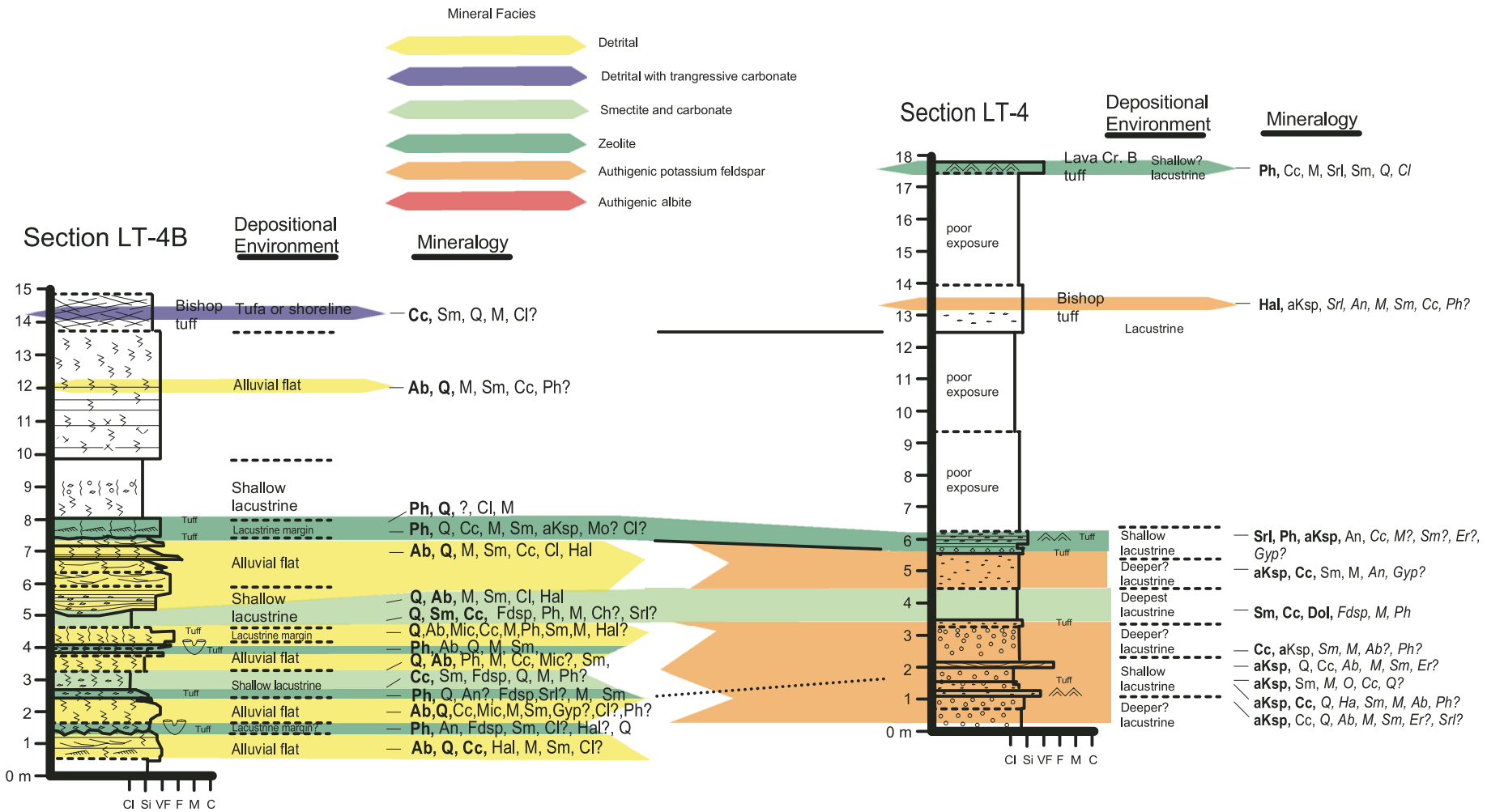

Figure 10. Color overlay of mineralogical facies along cross-section C-C' including sections LT-4B and LT-4. See Plate 2 caption for mineral abbreviations. See Fig. 3 for grain size abbreviations.

brine within the basin is retarded. In basins with relatively low topographic relief and low upland recharge, the resulting R_a is higher and free convection is promoted.

Rogers and Dreiss (1995a, 1995b) examined saline groundwater distributions at Mono Lake, California, a modern saline, alkaline lake in a closed hydrologic basin, using numerical simulations and modern hydrologic data. Their results confirm Duffy and Al-Hassan's (1988) observations for low lake-level conditions, but show depression of the central basin brine beneath the sediment-water interface during high lake conditions. Subsequent falling lake levels resulted in return of the brine to the surface and greatly increased solute contents. Time scales of buoyant equilibration of the brine at Mono Lake are hundreds to thousands of years, suggesting that only the effects of relatively long-term lake-level changes affect such changes in saline groundwater movement.

Another key consideration is the variation in effective moisture in the Lake Tecopa basin during the Pleistocene and attendant effects on lake levels. Lake Tecopa underwent an overall increase in lake level through early to middle Pleistocene punctuated by shorter-lived highstands (Morrison, 1991; 1999), most of which correlate with regional climatic events. Although the overall trend may relate to increased drainage basin area through time and hydrographic effects of regional uplift (e.g., Winograd et al., 1985), the shorter-term events are best related to regional arid-humid cycles of varying period (Smith, 1984; Winograd et al., 1992; Morrison, 1999; Tchakerian and Lancaster, 2002). Morrison (1999) estimated that during the last highstand (180 ka, isotope stage 6) temperatures at Tecopa were 10.5 °C lower than the present mean annual temperature of 19.5 °C and mean annual precipitation was 20–25 cm as compared to the modern value of 7 cm. These cooler and wetter conditions created conditions favoring higher water tables throughout the region (Quade et al., 1995, 2003; Nelson et al., 2001). Changes in spring discharge also changed the hydrology of the basin, such that intervening ranges (e.g., Nopah Range, Resting Spring Range) may have become significant recharge sources for the Tecopa basin. Thus, the proximity of recharge sources may have changed from regional during arid settings, such as today, to local during more humid settings.

Based on the observed Pliocene to middle Pleistocene lake-level record at Lake Tecopa and hypsometry of the Tecopa basin, saline groundwater within the basin would have likely undergone free convection during low lake-level events (Fig. 11). Assuming that groundwater flow is similar to today and dominated by regional, interbasin flow (Winograd and Thordarson, 1975; Thomas et al., 1996; Larsen et al., 2001), the characteristic length scale (L) (parameters defined in Duffy and Al-Hassan, 1988) for the basin is 40 km (distance to Spring Mountains, a regional recharge source), whereas the characteristic depth scale (D) is ~1.1 km (based on geophysical model from Louie et al., 2001). Assuming a length scale of 40 km, a recharge zone length (σ) of ~35 km, a discharge zone length of ~5 km, and a salt-nose length (L_o) of as much as 1 km, the position of the salt nose in the interbasin flow system (Duffy and Al-Hassan, 1988) is given by:

$$L_o^* = [L_o/L][\sigma/(L - \sigma)]^{1/2}[L/D]^{3/2} \sim 10. \quad (3)$$

Linear correlation of L_o^* to the Rayleigh number suggests a value of ~3000 (Fig. 15 of Duffy and Al-Hassan, 1988), well above Duffy and Al-Hassan's (1988) empirical threshold for free convection of R_a ~400–600. The above calculations assume that a hydrologic steady state was reached in the basin, which is likely to have taken thousands or more years to achieve, depending on the gradient and overall hydraulic conductivity in the fractured carbonate and basin-fill aquifers. Assuming that steady state was reached, the central brine would have slowly circulated through ashes, sands, and silts within the center of the basin, reacting with previously existing detrital and authigenic minerals to create the observed authigenic feldspar mineral facies.

During the highest levels of Lake Tecopa, recorded by the green smectite-carbonate facies mudstones, lake water filled the valley to near the bedrock margins of the basin (Fig. 11). Such conditions reduce potential for groundwater circulation in the basin through both decreased salinity contrast between fresh groundwater and brackish basin-fill water, as well as decrease in the width of recharge and discharge zones (Duffy and Al-Hassan, 1988). Assuming that local flow dominated during humid conditions, the characteristic L for the basin would be 5 km (distance to Nopah Range, a local recharge source) and the characteristic D would be ~1.1 km. Assuming a σ of ~4.5 km, a discharge zone length of ~0.5 km, and an L_o of as much as 0.25 km, the position of the salt nose in the interbasin flow system (Duffy and Al-Hassan, 1988) is given by:

$$L_o^* = [L_o/L][\sigma/(L - \sigma)]^{1/2}[L/D]^{3/2} \sim 1. \quad (4)$$

Linear correlation of L_o^* to the Rayleigh number suggests a value of ~400 (Fig. 15, Duffy and Al-Hassan, 1988), which is at the low end of Duffy and Al-Hassan's (1988) empirical threshold for free convection of R_a ~400–600. Assuming that equilibrium was reached during these conditions, groundwater circulation in the basin would be limited.

During these periods, relatively fresh or brackish waters overlay and likely depressed the central saline brine similar to that inferred by simulations in the Mono Basin (Rogers and Dreiss, 1995b), limiting reaction with near-surface sediments. Thus, the carbonate and Mg-clay mineral composition reflects reactions of detrital clay and ash with relatively dilute saline, alkaline waters, perhaps similar to that observed in Lake Turkana (Yuretich and Cerling, 1983). Because of the fine grain size and clay-rich mineralogy, subsequent low lake levels and initiation of free convection would likely only overprint sediments within the center of the basin.

The groundwater circulation model described above accords well with observations in other saline, alkaline lake deposits, such as the Magadi beds in East Africa and intervals of the Green River Formation in Wyoming, USA. Previous reviews of saline, alkaline lake deposits have commented on the absence of lateral zoning of authigenic silicate minerals in narrow, deep basins and the prevalence of lateral zonation in broad, shallow basins (Surdam, 1977; Eugster, 1986; Langella et al., 2001). Furthermore, vertical brine migration has been inferred in the diagenetic interpretation of parts of the Laney Member of the Green River Formation (Ratterman and Surdam, 1981) and lacustrine intervals and underlying sandstones of the Upper Jurassic Morrison Formation in southwestern Colorado, U.S. (Turner and Fishman, 1998), both of which represent authigenesis in broad shallow basins. Examples of vertical authigenic silicate mineral distributions are limited to the Magadi Beds (Eugster, 1986) and possibly the Jurassic Newark Basin, New Jersey and Pennsylvania, U.S. (Smoot, 2006). The fundamental hydrologic differences between these systems are the relative magnitudes of topographic versus buoyancy drives for groundwater flow. In relatively flat, shallow groundwater flow systems, low hydraulic gradients allow for reversal of flow of dense groundwater, creating an opportunity for brines to cycle through the basinal sediments. Whereas in relatively steep, deep groundwater flow systems, the topographic drive forces the dense groundwater to the surface and the center of the basin (Duffy and Al-Hassan, 1988). For the Tecopa basin, brine circulation was favored under all but the highest lake-level conditions, although during those times less dense lake water depressed the underlying brine and limited reaction with surface sediments.

CONCLUSIONS AND APPLICATION

The Pliocene–Pleistocene Lake Tecopa beds represent deposits in and around an ancient perennial saline, alkaline lake. During most of the history recorded in the lake beds, sedimentation occurred in fluvial, deltaic, alluvial-fan, alluvial-flat, and eolian environments around the relatively shallow perennial lake. Saline, alkaline water chemistry is indicated by gaylussite molds and calcite pseudomorphs after trona in lacustrine mudstone, zeolite and alkali feldspar alteration of lacustrine mudstone, siltstone, and sandstone, and interbedded flaggy magadiite-type chert beds. Extensive mudflats were only present during a protracted early Pleistocene lowstand. Spring activity is evident in the deltaic, alluvial-flat, and alluvial-fan environments, often aligned along inferred faults. The sedimentary environments represented by the Lake Tecopa beds varied through time, but are similar to those present in and around saline, alkaline Lakes Bogoria and Magadi in East Africa. Eolian processes are suspected to have been important agents of sedimentation in the Tecopa basin that distinguish it from the east African lakes and many Pleistocene Great Basin pluvial lake basins.

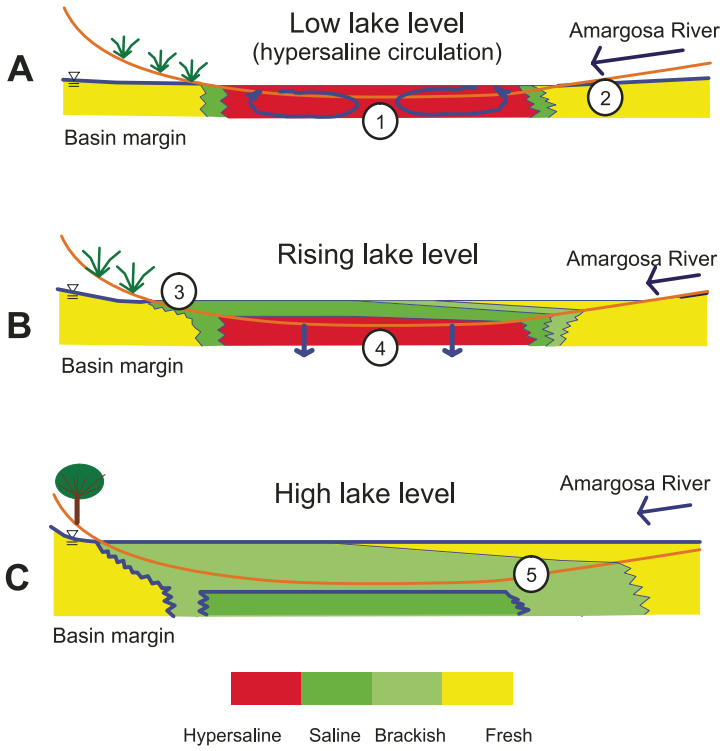

Figure 11. Summary diagram illustrating the effect of changing lake level on brine circulation, pore-water salinity, and associated diagenetic reactions in the Tecopa basin. Orange line represents land surface; vegetation is schematic. Upper blue line is lake surface or water table, as appropriate. (A) Arid conditions with shallow lake and mudflats; precipitation of trona and gaylussite in lake and magadiite and associated minerals on mudflats. (1) Density-driven circulation of hypersaline water in center of basin with surrounding mudflats that are periodically flooded; reaction of both detrital and earlier formed zeolites and clays to authigenic potassium feldspar and albite mineral facies. (2) Relatively fresh groundwater in adjacent alluvial and alluvial-flat environments; pedogenic carbonate and gypsum precipitation along with hydration and dioctahedral smectite formation on volcanic glass. (B) Rising lake-level conditions associated with pluvial onset; freshening of lake water, but still extensive gaylussite precipitation. (3) Saline lake water transgresses upon the alluvial flat and drowns Amargosa delta; dolomitization of pedogenic carbonate, clay mineral reactions (trioctahedral clay formation from detrital and earlier formed volcanogenic smectite) and zeolitization of tuffaceous lake-margin and shallow lacustrine deposits. (4) Overlying lake water mass pushes hypersaline water downward in basin fill; potential for retrograde reaction of potassium feldspar and albite facies to form zeolites(?). (C) High lake level associated with full pluvial conditions. (5) Deposition of extensive greenish-gray mudstone across the basin in contact with brackish to fresh lake water; calcite and dolomite precipitation in lake along with formation of trioctahedral smectite from solution and detrital clays.

Lake level varied in Lake Tecopa during the Pliocene and Pleistocene with a general progression toward higher lake levels through time. The earliest records indicate low to intermediate lake levels prior to the Huckleberry Ridge ash (2.02 Ma), followed by an interval of very low lake levels until ca. 1.0 Ma. Lake levels rose progressively during the middle Pleistocene, with most highstands corresponding to other lakes in the southwestern Great Basin region. The progressive increase in lake level through the Pleistocene seems generally consistent with effects from an increase in drainage basin area and regional uplift of the Sierra Nevada. The specific highstands, especially those in the middle Pleistocene, appear to correspond to humid climatic events in the region.

Authigenic silicate mineral precipitation and alteration appear to have been concurrent with sedimentation and reflect a complex interplay of depositional, geochemical, and hydrologic processes. Lacustrine mudstone, siltstone, sandstone, and tuff contain a variety of authigenic minerals, including alkali zeolites, trioctahedral smectite, authigenic feldspars, searlesite, and opal C-T, that have been interpreted in terms of five mineral facies. Changes in authigenic silicate mineralogy in sediments along the basin margin generally show good correspondence between depositional environment (short-term lake-level change) and mineralogy: alluvial-flat and fluvial deposits tend to show limited silicate mineral authigenesis (mainly detrital minerals plus smectite), whereas lacustrine margin to shallow lacustrine deposits show various degrees of zeolite authigenesis. However, sediment composition plays a role in that nonlacustrine sediments rich in volcanic ash tend to be altered to zeolites as well.

Authigenic mineralogy of sediments in the central basin commonly shows some remnant of depositional control, but is mainly affected by a secondary overprint by potassium feldspar, illite, and searlesite formed by chemical interaction with a circulating brine that rose and sank antithetically with long-term lake-level change. Remnants of the depositional facies include the smectite and carbonate minerals in some green mudstones as well as the sodic (authigenic albite) composition of the altered mudflat deposits. The authigenic mineralogy of the basin center environments can be interpreted by considering hydrodynamics of brine migration under differing hydroclimatic conditions in the Tecopa basin. During low lake levels driven by arid conditions and regional groundwater flow, basin-central brines rise to the surface and circulate through

near-surface sediments. In contrast, during high lake levels driven by humid climatic conditions and local groundwater flow, the brine is displaced downward and circulation is limited.

The results from the Tecopa basin have implications for the utility of authigenic silicate mineral distributions in deciphering ancient lake levels and thus paleohydrology. In broad, shallow, saline, alkaline lake basins, such as Tecopa, initial authigenic mineralogy controlled by short-term lake-level changes is likely to be best preserved in basin-margin areas, whereas sediments in basin-central regions may be more complexly affected by brines. In deeper basins with surrounding high mountains, such as rift basins, the authigenic mineral records in the basin center may reflect more faithfully the lake-level record. Other factors, such as hydraulic conductivity of basinal sediments, recharge and runoff considerations, and the age and continuity of the lake basin may further affect the importance of brine migration.

ACKNOWLEDGMENTS

I thank Terry Pavlis and Laura Serpa (University of New Orleans) at the Shoshone Education and Research Center for providing local accommodations and many good meals. Benny Troxel and Lauren Wright provided many research contacts, locations with interesting features, and words of encouragement. Several students and colleagues have contributed extensively to this work, either in the lab or the field, including Derrick McNeal, Cathy Ratcliff, Philip Davis, Jeff Knott, George Swihart, Rhonda Yates, and Jamie Woods. I appreciate the helpful reviews by Greg Mack and Daniel Deocampo, both of whom significantly improved the presentation and interpretation of this work. This study was partially supported by a University of Memphis Faculty Research Grant and the United States Geological Survey.

REFERENCES CITED

Anderson, D.E., Poths, J., and Wells, S.G., 1994, Cosmogenic ^{3}He ages of wave-cut scarps in the Lake Tecopa basin of SE California: Implications for sampling strategy and the age consistency of isochronous surfaces: Eos (Transactions, American Geophysical Union), v. 75, p. 288.

Ashley, G.M., and Driese, S.G., 2000, Paleopedology and paleohydrology of a volcaniclastic paleosol interval: Implications for early Pleistocene stratigraphy and paleoclimate record, Olduvai Gorge, Tanzania: Journal of Sedimentary Research, v. 70, p. 1065–1080, doi: 10.1306/040300701065.

Banfield, J.F., Jones, B.F., and Veblen, D.R., 1991, An AEM-TEM study of weathering and diagenesis, Abert Lake, Oregon: II. Diagenetic modification of the sedimentary assemblage: Geochimica et Cosmochimica Acta, v. 55, p. 2795–2810, doi: 10.1016/0016-7037(91)90445-B.

Bellanca, A., Calvo, J.P., Censi, P., Neri, R., and Pozo, M., 1992, Recognition of lake-level changes in Miocene lacustrine units, Madrid Basin, Spain. Evidence from facies analysis, isotope geochemistry, and clay mineralogy: Sedimentary Geology, v. 76, p. 135–153, doi: 10.1016/0037-0738(92)90080-B.

Birkeland, P.W., 1999, Soils and geomorphology: New York, Oxford University Press, 430 p.

Born, S.M., 1972, Late Quaternary history, deltaic sedimentation, and mudlump formation at Pyramid Lake, Nevada: Reno, Nevada, Desert Research Institute, 97 p.

Bowers, T.S., and Burns, R.G., 1990, Activity diagrams for clinoptilolite: Susceptibility of this zeolite to further diagenetic reactions: American Mineralogist, v. 75, p. 601–619.

Chipera, S.J., and Apps, J.A., 2001, Geochemical stability of natural zeolites, *in* Bish, D.L., and Ming, D.W., eds., Natural zeolites: Occurrence, properties, applications: Reviews in Mineralogy and Geochemistry, v. 45, p. 117–162.

Claassen, H.C., 1985, Sources and mechanisms of recharge for groundwater in the west-central Amargosa Desert, Nevada—A geochemical interpretation: U.S. Geological Survey Professional Paper 712-F, 31 p.

Cohen, A.S., 2003, Paleolimnology: New York, Oxford University Press, 500 p.

Deocampo, D.M., 2004, Authigenic clays in East Africa: Regional trends and paleolimnology at the Plio-Pleistocene boundary, Olduvai Gorge, Tanzania: Journal of Paleolimnology, v. 31, p. 1–9, doi: 10.1023/B:JOPL.0000013353.86120.9b.

Deocampo, D.M., and Ashley, G.M., 1999, Siliceous islands in a carbonate sea: Modern and Pleistocene spring-fed wetlands in Ngorongoro crater and Olduvai Gorge, Tanzania: Journal of Sedimentary Research, v. 69, p. 974–979.

Deocampo, D.M., Blumenschine, R.J., and Ashley, G.M., 2002, Wetland diagenesis and traces of early hominids, Olduvai Gorge, Tanzania: Quaternary Research, v. 57, p. 271–281, doi: 10.1006/qres.2001.2317.

Dibble, W.E., Jr., and Tiller, W.A., 1981, Non-equilibrium water/rock interactions—I. Model for interface-controlled reactions: Geochimica et Cosmochimica Acta, v. 45, p. 79–92, doi: 10.1016/0016-7037(81)90265-9.

Dohrenwend, J.C., Bull, W.B., McFadden, L.D., Smith, G.I., Smith, R.S.U., and Wells, S.G., 1991, Quaternary geology of the Basin and Range Province in California, *in* Morrison, R.B., ed., Quaternary nonglacial geology, conterminous U.S.: Boulder, Colorado, Geological Society of America, Geology of North America, v. K-2, p. 321–352.

Drever, J.I., 1973, The preparation of oriented clay mineral specimens for X-ray diffraction analysis by a filter-membrane peel technique: American Mineralogist, v. 58, p. 553–554.

Duffy, C.J., and Al-Hassan, S., 1988, Groundwater circulation in a closed desert basin: Topographic scaling and climatic forcing: Water Resources Research, v. 24, p. 1675–1688, doi: 10.1029/WR024i010p01675.

Eugster, H.P., 1970, Chemistry and origin of the brines of Lake Magadi, *in* Fiftieth Anniversary Symposia, Mineralogy and Geochemistry of Non-Marine Evaporites: Mineralogical Society of America Special Paper 3, p. 213–235.

Eugster, H.P., 1980, Lake Magadi, Kenya, and its precursors, *in* Nissenbaum, A., ed., Hypersaline brines and evaporitic environments: New York, Elsevier Scientific Publishing Company, p. 195–232.

Eugster, H.P., 1986, Lake Magadi, Kenya: A model for rift valley hydrochemistry and sedimentation?, *in* Frostick, L.E., ed., Sedimentation in the African rifts: Geological Society [London] Special Publication 25, p. 177–89.

Eugster, H.P., and Hardie, L.A., 1978, Saline lakes, *in* Lerman, A., ed., Chemistry, geology, and physics of lakes: New York, Springer-Verlag, p. 237–293.

Gude, A.J., III, and Sheppard, R.A., 1986, Magadi-type chert—A distinctive diagenetic variety from lacustrine deposits, *in* Mumpton, F.A., ed., Studies in diagenesis: U.S. Geological Survey Bulletin 1578, p. 335–346.

Gustavson, T.C., 1991, Buried vertisols in a lacustrine facies of the Pliocene Fort Hancock Formation, Hueco Bolson, west Texas and Chihuahua, Mexico: Geological Society of America Bulletin, v. 103, p. 448–460, doi: 10.1130/0016-7606(1991)103<0448:BVILFO>2.3.CO;2.

Hardie, L.A., and Eugster, H.P., 1970, The evolution of closed basin brines, *in* Fiftieth Anniversary Symposia, Mineralogy and Geochemistry of Non-Marine Evaporites: Mineralogical Society of America Special Paper 3, p. 273–290.

Hasiotis, S.T., 2002, Continental trace fossils: Society for Sedimentary Geology (SEPM) Short Course Notes no. 51, 132 p.

Hawkins, D.B., 1981, Kinetics of glass dissolution and zeolite formation under hydrothermal conditions: Clays and Clay Minerals, v. 29, p. 331–340, doi: 10.1346/CCMN.1981.0290503.

Hawkins, D.B., Sheppard, R.A., and Gude, A.J., III, 1978, Hydrothermal synthesis of clinoptilolite and comments on the assemblage phillipsite-clinoptilolite-mordenite, *in* Sand, L.B., and Mumpton, F.A., eds., Natural zeolites, occurrence, properties, use: Oxford, Pergamon Press, p. 337–344.

Hay, R.L., 1966, Zeolites and zeolitic reactions in sedimentary rocks: Geological Society of America Special Paper 85, 130 p.

Hay, R.L., 1968, Chert and its sodium-silicate precursors in sodium-carbonate lakes of east Africa: Contributions to Mineralogy and Petrology, v. 17, p. 255–274, doi: 10.1007/BF00380740.

Hay, R.L., 1976, Geology of the Olduvai Gorge: Berkeley, University of California Press, 203 p.

Hay, R.L., and Kyser, T.K., 2001, Chemical sedimentology and paleoenvironmental history of Lake Olduvai, a Pliocene lake in northern Tanzania: Geological Society of America Bulletin, v. 113, p. 1505–1521, doi: 10.1130/0016-7606(2001)113<1505:CSAPHO>2.0.CO;2.

Hay, R.L., Pexton, R.E., Teague, T.T., and Kyser, T.K., 1986, Spring-related carbonate rocks, Mg clays, associated minerals in Pliocene deposits of the Amargosa Desert, Nevada and California: Geological Society of America Bulletin, v. 97, p. 1488–1503, doi: 10.1130/0016-7606(1986)97<1488:SCRMCA>2.0.CO;2.

Hillhouse, J.W., 1987, Late Tertiary and Quaternary geology of the Tecopa basin, southeastern California: U.S. Geological Survey Miscellaneous Investigations Map I-1728, 16 p.

Hover, V., and Ashley, G.M., 2003, Geochemical signatures of paleodepositional and diagenetic environments: A STEM/AEM study of authigenic clay minerals from an arid rift basin, Olduvai Gorge, Tanzania: Clays and Clay Minerals, v. 51, p. 231–251, doi: 10.1346/CCMN.2003.0510301.

Ingles, M., Salvany, J.M., Muñoz, A., and Pérez, A., 1998, Relationship of mineralogy to depositional environments in the non-marine Tertiary mudstones of the southwestern Ebro Basin (Spain): Sedimentary Geology, v. 116, p. 159–176, doi: 10.1016/S0037-0738(97)00112-7.

Jannik, N.O., Phillips, F.M., Smith, G.I., and Elmore, D., 1991, A ^{36}Cl chronology of lacustrine sedimentation in the Pleistocene Owens River system: Geological Society of America Bulletin, v. 103, p. 1146–1159, doi: 10.1130/0016-7606(1991)103<1146:ACCOLS>2.3.CO;2.

Jones, B.F., 1966, Geochemical evolution of closed basin waters in the western Great Basin, *in* Rau, J.L., ed., Second symposium on salt, Volume 1: Cleveland, Northern Ohio Geological Society, p. 181–200.

Jones, B.F., and Deocampo, D.M., 2003, Geochemistry of saline lakes, *in* Drever, J.I., ed., Surface and ground water, weathering, erosion, and soils: Treatise on Geochemistry, Volume 5: New York, Elsevier, p. 393–424.

Jones, B.F., and Weir, A.H., 1983, Clay minerals of Lake Abert, an alkaline, saline, lake: Clays and Clay Minerals, v. 31, p. 161–172, doi: 10.1346/CCMN.1983.0310301.

Khoury, H.N., Eberl, D.D., and Jones, B.F., 1982, Origin of magnesium clays from the Amargosa Desert, Nevada: Clays and Clay Minerals, v. 30, p. 327–336, doi: 10.1346/CCMN.1982.0300502.

Langbein, W.B., 1961, Salinity and hydrology of closed lakes: U.S. Geological Survey Professional Paper 412, 20 p.

Langella, A., Cappelletti, P., and de Gennaro, M., 2001, Zeolites in closed hydrologic systems, *in* Bish, D.L., and Ming, D.W., eds., Natural zeolites: Occurrence, properties, applications: Reviews in Mineralogy and Geochemistry, v. 45, p. 235–260.

Larsen, D., 1997, Relationships between depositional facies and authigenic minerals in the Plio-Pleistocene Lake Tecopa Beds, southeastern California: Geological Society of America Abstracts with Programs, v. 29, no. 6, p. 437.

Larsen, D., 2000, Sedimentology and stratigraphy of the Plio-Pleistocene Lake Tecopa beds, southeastern California: A work in progress: San Bernardino County Museum Association Quarterly, v. 47, p. 56–62.

Larsen, D., Swihart, G.H., and Xiao, Y., 2001, Hydrochemistry and isotopic composition of springs in the Tecopa basin, southeastern California, U.S.A: Chemical Geology, v. 179, p. 17–35, doi: 10.1016/S0009-2541(01)00313-8.

Larsen, D., Knott, J., and Jayko, A., 2003, Comparison of middle Pleistocene records in Death, Panamint, and Tecopa valleys, California: Implications for regional

climate: Geological Society of America Abstracts with Programs, v. 35, no. 6, p. 333.

Larson, E.E., and Patterson, P.E., 1993, The Matuyama-Bruhnes reversal at Tecopa basin, southeastern California, revisited again: Earth and Planetary Science Letters, v. 120, p. 311–325, doi: 10.1016/0012-821X(93)90247-7.

Larson, E.E., Patterson, P.E., and Luiszer, F., 1991, Paleoclimatic record from 2.4 to 0.5 Ma, Tecopa basin, southeastern California: Geological Society of America Abstracts with Programs, v. 23, no. 5, p. 120.

Louie, J.N., Cetintas, A., Chekuri, V., Corchuelo, W.D., Lei, Y., Li, L., Mekala, G., Ozalaybey, S., Raskulinecz, J., and Morrison, R.B., 2001, Geophysical constraints on the cessation of extension and thickness of basin fill in Tecopa Valley, California: http://www.seismo.unr.edu/ftp/pub/louie/papers/tecopa/tecopa.html.

Mack, G.H., Seager, W.R., and Kieling, J., 1994, Late Oligocene and Miocene faulting and sedimentation and evolution of the southern Rio Grande Rift, New Mexico, USA: Sedimentary Geology, v. 92, p. 79–96, doi: 10.1016/0037-0738(94)90055-8.

Mack, G.H., Cole, D.R., and Trevino, L., 2000, The distribution and discrimination of shallow, authigenic carbonate in the Pliocene-Pleistocene Palomas Basin, southern Rio Grande Rift: Geological Society of America Bulletin, v. 112, p. 643–656, doi: 10.1130/0016-7606(2000)112<0643:TDADOS>2.3.CO;2.

Mariner, R.H., and Surdam, R.C., 1970, Alkalinity and formation of zeolites in saline alkaline lakes: Science, v. 170, p. 977–980, doi: 10.1126/science.170.3961.977.

Mifflin, M.D., 1988, Region 5, Great Basin, *in* Back, W., et al., eds., Hydrogeology: Boulder, Colorado, Geological Society of America, Geology of North America, v. O-2, p. 69–78.

Moore, D.M., and Reynolds, R.C., Jr., 1989, X-ray diffraction and the identification and analysis of clay minerals: New York, Oxford University Press, 332 p.

Morrison, R.B., 1991, Quaternary stratigraphic, hydrologic, and climatic history of the Great Basin, with emphasis on Lakes Lahontan, Bonneville, and Tecopa, *in* Morrison, R.B., ed., Quaternary non-glacial history, conterminous U.S.: Boulder, Colorado, Geological Society of America, Geology of North America, v. K-2, p. 283–320.

Morrison, R.B., 1999, Lake Tecopa: Quaternary geology of Tecopa valley, California, a multimillion-year record and its relevance to the proposed nuclear-waste repository at Yucca Mountain, Nevada, *in* Wright, L.A., and Troxel, B.W., eds., Cenozoic basins of the Death Valley region: Geological Society of America Special Paper 333, p. 301–344.

Mozley, P.S., and Davis, J.M., 2005, Internal structure and mode of growth of elongate calcite concretions: Evidence for small-scale, microbially induced, chemical heterogeneity in groundwater: Geological Society of America Bulletin, v. 117, p. 1400–1412, doi: 10.1130/B25618.1.

Nelson, S.T., Karlsson, H.R., Paces, J.B., Tingey, D.G., Ward, S., and Peters, M.T., 2001, Paleohydrologic record of spring deposits in and around Pleistocene pluvial Lake Tecopa, southeastern California: Geological Society of America Bulletin, v. 113, p. 659–670, doi: 10.1130/0016-7606(2001)113<0659:PROSDI>2.0.CO;2.

Picard, M.D., and High, L.R., Jr., 1973, Sedimentary structures of ephemeral streams: Developments in Sedimentology 17: Amsterdam, Elsevier, 223 p.

Quade, J., Mifflin, M.D., Pratt, W.L., McCoy, W., and Burckle, L., 1995, Fossil spring deposits in the southern Great Basin and their implications for changes in water-table levels near Yucca Mountain, Nevada, during Quaternary time: Geological Society of America Bulletin, v. 107, p. 213–230, doi: 10.1130/0016-7606(1995)107<0213:FSDITS>2.3.CO;2.

Quade, J., Forester, R.M., and Whelan, J.F., 2003, Late Quaternary paleohydrology and paleotemperature change in southern Nevada, *in* Enzel, Y., et al., eds., Paleoenvironments and paleohydrology of the Mojave and Southern Great Basin: Geological Society of America Special Paper 368, p. 165–188.

Ratterman, N.G., and Surdam, R.C., 1981, Zeolite mineral reactions in a tuff in the Laney member of the Green River Formation, Wyoming: Clays and Clay Minerals, v. 29, p. 365–377, doi: 10.1346/CCMN.1981.0290506.

Remy, R.R., and Ferrell, R.E., 1989, Distribution and origin of analcime in marginal lacustrine mudstones of the Green River Formation, south-central Uinta Basin, Utah: Clays and Clay Minerals, v. 37, p. 419–432, doi: 10.1346/CCMN.1989.0370505.

Renaut, R.W., 1993, Zeolitic diagenesis of late Quaternary fluviolacustrine sediments and associated calcrete formation in the Lake Bogoria Basin, Kenya Rift valley: Sedimentology, v. 40, p. 271–301, doi: 10.1111/j.1365-3091.1993.tb01764.x.

Renaut, R.W., and Tiercelin, J.-J., 1994, Lake Bogoria, Kenya Rift Valley—A sedimentological overview, *in* Renaut, R.W. and Last, W.M., eds., Sedimentology and geochemistry of modern and ancient saline lakes: Society for Sedimentary Geology (SEPM) Special Publication 50, p. 101–124.

Reynolds, R.E., 1991, The Shoshone zoo: A Ranchlabrean assemblage from Tecopa, *in* Reynolds, R.E., ed., Crossing the borders: Quaternary studies in eastern California and southwestern Nevada: Redlands, California, San Bernardino County Museum Special Publication, p. 158–162.

Rogers, D.B., and Dreiss, S.J., 1995a, Saline groundwater in Mono Basin, California: 1: Distribution: Water Resources Research, v. 31, p. 3131–3150, doi: 10.1029/95WR02108.

Rogers, D.B., and Dreiss, S.J., 1995b, Saline groundwater in Mono Basin, California: 2. Long-term control of lake salinity by groundwater: Water Resources Research, v. 31, p. 3151–3169, doi: 10.1029/95WR02109.

Rosen, M.R., 1994, The importance of groundwater in playas: A review of playa classifications and the sedimentology and hydrology of playas, *in* Rosen, M.R., ed., Paleoclimate and basin evolution of playa systems: Geological Society of America Special Paper 289, p. 1–18.

Sarna-Wojcicki, A.M., Morrison, S.D., Meyer, C.E., and Hillhouse, J.W., 1987, Correlation of upper Cenozoic tephra layers between sediments of the western United States and eastern Pacific Ocean and comparison with biostratigraphic and magnetostratigraphic age data: Geological Society of America Bulletin, v. 98, p. 207–223, doi: 10.1130/0016-7606(1987)98<207:COUCTL>2.0.CO;2.

Sheppard, R.A., 1994, Zeolitic diagenesis of tuffs in Miocene lacustrine rocks near Harney Lake, Harney County, Oregon: U.S. Geological Survey Bulletin 2108, 21 p.

Sheppard, R.A., and Gude, A.J., III, 1968, Distribution and genesis of authigenic silicate minerals in tuffs of Pleistocene Lake Tecopa, Inyo County, California: U.S. Geological Survey Professional Paper 597, 38 p.

Sheppard, R.A., and Gude, A.J., III, 1969, Diagenesis of tuffs in the Barstow Formation, Mud Hills, San Bernardino County, California: U.S. Geological Survey Professional Paper 634, 35 p.

Sheppard, R.A., and Gude, A.J., III, 1973, Zeolites and associated silicate minerals in tuffaceous rocks of the Big Sandy Formation, Mohave County, Arizona: U.S. Geological Survey Professional Paper 830, 36 p.

Sheppard, R.A., and Hay, R.L., 2001, Occurrence of zeolites in sedimentary rocks: An overview, *in* Bish, D.L., and Ming, D.W., eds., Natural zeolites: Occurrence, properties, applications: Reviews in Mineralogy and Geochemistry, v. 45, p. 217–234.

Smith, G.I., 1984, Paleohydrologic regimes in the southwestern Great Basin, 0–3.2 m.y. ago, compared with other long records of "global" climate: Quaternary Research, v. 22, p. 1–17, doi: 10.1016/0033-5894(84)90002-4.

Smoot, J.P., 2006, Late Triassic lacustrine evaporite minerals of the Newark basin, New Jersey and Pennsylvania: Geological Society of America Abstracts with Programs, v. 38, no. 7, p. 85.

Smoot, J.P., and Lowenstein, T.K., 1991, Depositional environments of nonmarine evaporates, *in* Melvin, J.L., ed., Evaporites, petroleum, and mineral resources: Amsterdam, Elsevier, p 189–347.

Starkey, H.C., and Blackmon, P.D., 1979, Clay mineralogy of Pleistocene Lake Tecopa, Inyo County, California: U.S. Geological Survey Professional Paper 1061, 34 p.

Street-Perrott, F.A., and Harrison, S.P., 1985, Lake levels and climate reconstruction, *in* Hecht, A.D., ed., Paleoclimate analysis and modeling: New York, John Wiley and Sons, p. 291–340.

Surdam, R.C., 1977, Zeolites in closed hydrologic systems, *in* Mumpton, F.A., ed., Mineralogy and geology of natural zeolites: Mineralogical Society of America Reviews in Mineralogy, v. 4, p. 65–92.

Surdam, R.C., and Eugster, H.P., 1976, Mineral reactions in the sedimentary deposits of the Lake Magadi region, Kenya: Geological Society of America Bulletin, v. 87, p. 1739–1752, doi: 10.1130/0016-7606(1976)87<1739:MRITSD>2.0.CO;2.

Surdam, R.C., and Parker, R.D., 1972, Authigenic aluminosilicate minerals in the tuffaceous rocks of the Green River Formation, Wyoming: Geological Society of America Bulletin, v. 83, p. 689–700, doi: 10.1130/0016-7606(1972)83[689:AAMITT]2.0.CO;2.

Surdam, R.C., and Sheppard, R.A., 1978, Zeolites in saline, alkaline-lake deposits, *in* Sand, L.B., and Mumpton, F.A., eds., Natural zeolites, occurrence, properties, use: Oxford, Pergamon Press, p. 145–174.

Taylor, M.W., and Surdam, R.C., 1981, Zeolite reactions in the tuffaceous sediments at Teels Marsh, Nevada: Clays and Clay Minerals, v. 29, p. 341–352, doi: 10.1346/CCMN.1981.0290504.

Tchakerian, V.P., and Lancaster, N., 2002, Late Quaternary arid/humid cycles in the Mojave Desert and western Great Basin of North America: Quaternary Science Reviews, v. 21, p. 799–810, doi: 10.1016/S0277-3791(01)00128-7.

Thomas, J.M., Welch, A.H., and Dettinger, M.D., 1996, Geochemistry and isotope hydrology of representative aquifers in the Great Basin Region of Nevada, Utah, and adjacent states: U.S. Geological Survey Professional Paper 1409-C, 100 p.

Turner, C.E., and Fishman, N.S., 1991, Jurassic Lake T'oo'dichi': A large alkaline, saline lake, Morrison Formation, eastern Colorado Plateau: Geological Society of America Bulletin, v. 103, p. 538–558, doi: 10.1130/0016-7606(1991)103<0538:JLTODA>2.3.CO;2.

Turner, C.E., and Fishman, N.S., 1998, Late Jurassic lacustrine deposits and implications for paleohydrology: deposition to early compaction, *in* Pitman, J.K., and Carroll, A.R., eds., Modern and ancient lake systems: Salt Lake City, Utah Geological Survey, p. 31–49.

Valet, J.-P., Tauxe, L., and Clark, D.R., 1988, The Matuyama-Brunhes transition recorded from Lake Tecopa sediments (California): Earth and Planetary Science Letters, v. 87, p. 463–472, doi: 10.1016/0012-821X(88)90009-X.

Winograd, I.J., and Thordarson, W., 1975, Hydrogeologic and hydrochemical framework, south-central Great Basin, Nevada-California, with special reference to the Nevada Test Site: U.S. Geological Survey Professional Paper 712-C, 126 p.

Winograd, I.J., Szabo, B.J., Coplen, T.B., Riggs, A.C., and Kolesar, P.T., 1985, Two million year record of deuterium depletion in Great Basin ground waters: Science, v. 227, p. 519–522, doi: 10.1126/science.227.4686.519.

Winograd, I.J., Coplen, T.B., Landwehr, J.M., Riggs, A.C., Ludwig, K.R., Szabo, B.J., Kolesar, P.T., and Revesz, K.M., 1992, Continuous 500,000-year climate record from vein calcite in Devils Hole, Nevada: Science, v. 258, p. 255–260, doi: 10.1126/science.258.5080.255.

Wirsching, U., 1976, Experiments on hydrothermal alteration processes of rhyolitic glass in closed and "open" system: Neues Jahrbuch für Minerologie Monatshefte, v. 5, p. 203–213.

Woodburne, M.O., and Whistler, D.P., 1991, The Tecopa Lake beds, *in* Reynolds, R.E., ed., Crossing the borders: Quaternary studies in eastern California and southwestern Nevada: Redlands, California, San Bernardino County Museum Special Publication, p. 155–157.

Yuretich, R.F., and Cerling, T.E., 1983, Hydrochemistry of Lake Turkana, Kenya: Mass balance and mineral reactions in an alkaline lake: Geochimica et Cosmochimica Acta, v. 47, p. 1099–1109, doi: 10.1016/0016-7037(83)90240-5.

Manuscript Received 5 September 2007
Revised Manuscript Received 10 February 2008
Manuscript Accepted 5 March 2008